Chapter 4
Reactive Power Compensation in Energy Transmission Systems with Sinusoidal and Nonsinusoidal Currents

Milan Stork and Daniel Mayer

Abstract A standout amongst the most noteworthy current talks in electrical designing is the meaning of the responsive power under nonsinusoidal conditions in nonlinear electric frameworks. New meanings of responsive power have been talked about in the most recent years. Despite the fact that the component of electric energy stream for nonsinusoidal conditions is all around depicted today, so toll is not yet accessible a summed up power hypothesis, and hypothetical figuring for the configuration of such gadgets as dynamic channels or element compensators. Thusly the undertaking of planning compensators for advance energy transmission with nonlinear time-fluctuating loads in nonsinusoidal administrations is, a long way from clear. Voltage and current harmonics created by nonlinear loads increment power losses in transmission frameworks and, in this manner, negatively affect effectivity of appropriation frameworks and parts. While a few harmonics are brought on by framework nonlinearities, for example, transformer immersion, most harmonic are delivered by power electronic loads, for example, flexible velocity drives and diode span rectifiers. In this chapter the reactive power compensation for sinusoidal and nonsinusoidal circumstances, where nonlinear circuit voltages and streams contain harmonic are explained and reenacted. The results can be used for control algorithms of automatic compensators which are also described. The main aim of this chapter is based on the dissipative systems theory and therefore theory of cyclodissipativity which can be used for calculation of compensation elements (capacitors, inductors) for reactive power compensation. The compensation elements are determined by minimizing line losses. It will show that approach base on dissipative systems theory provides an important mathematical framework for

M. Stork (✉)
Department of Applied Electronics and Telecommunications, University of West Bohemia, Plzen, Czech Republic
e-mail: stork@kae.zcu.cz

D. Mayer
Department of Theory of Electrical Engineering, University of West Bohemia, Plzen, Czech Republic
e-mail: mayer@kte.zcu.cz

N. Mahdavi Tabatabaei et al. (eds.), *Reactive Power Control in AC Power Systems*, Power Systems, DOI 10.1007/978-3-319-51118-4_4

analyzing and designing of compensators for reactive power compensation even for general nonlinear loads. The presented theory is supplemented by a series of examples and simulations.

4.1 Introduction

A standout amongst the hugest current examinations in electrical designing is the meaning of the reactive power (RP) under nonsinusoidal conditions in nonlinear electric frameworks. New meanings of RP have been talked about in the most recent years. Despite the fact that the component of electric energy stream for nonsinusoidal conditions is all around portrayed today, so admission is not yet accessible a summed up power hypothesis, and hypothetical computations for the configuration of such gadgets as dynamic channels or element compensators. In this manner, the undertaking of planning compensators for improve energy transmission with nonlinear time-changing loads in nonsinusoidal administrations is, a long way from clear. Voltage and current harmonics created by nonlinear loads increment power loss in transmission frameworks and, in this manner, negatively affect effectivity of conveyance frameworks and parts. While a few harmonics are created by framework nonlinearities, for example, transformer immersion, most harmonic are delivered by power electronic loads, for example, notice adjustable speed drives and diode span rectifiers. In this chapter the reactive power compensation for sinusoidal and nonsinusoidal circumstances, where voltages and streams contain harmonic are contemplated and mimicked. The outcomes can be utilized for control calculations of programmed compensators. The fundamental point of this section depends on the dissipative frameworks hypothesis and along these lines hypothesis of cyclodissipativity which can be utilized for estimation of compensation components (capacitors, inductors) for RP pay. It will demonstrate that approach base on dissipative frameworks hypothesis gives a numerical structure to breaking down and planning of compensators.

Reactive power investigation and compensation are significant for conveyed era and deregulation, which are the two primary procedures reshaping electric energy frameworks today. Conveyed era requires a portrayal of complex loads with bidirectional power streams, both in enduring state and in incessant homeless people. Deregulation requires exact evaluation of power streams, as well as of pay endeavors and different administrations that incorporates numerous members and chiefs.

Our inspiration is to think about inert power and probability of pay for energy frameworks. Today, the exchanging power converters can working at time interims much shorter than the key (50 or 60 Hz) period. Numerous broadly utilized outline instruments (e.g., those taking into account the idea of “quick reactive power”) are described solely in the time space. Their application once in a while results in presentation of harmonic that were not present in the first waveforms. This, thusly, might energize unmodeled progress, and bring about unsatisfactory drifters. The

specialized means for online pay of polyphase frameworks are simply getting to be accessible. This is valid for power electronic converters (e.g., voltage-sourced inverters with quick exchanging and short reaction times) furthermore for control equipment (e.g., reasonable miniaturized scale controllers with sign preparing ability).

Improving energy exchange from an air conditioner source to a load is an established issue in electrical designing. The outline of power frameworks is such that the exchange happens at the key frequency of the source. Practically speaking, the proficiency of this exchange is typically diminished because of the phase shift in the middle of voltage and current at the major frequency. The phase shift emerges to a great extent because of energy streams portraying electric engines. The power variable (PF), characterized as the proportion between the genuine or dynamic power (normal of the immediate power) and the clear power (the result of rms root mean square estimations of the voltage and current), then communicates the energy transmission proficiency for a given load. The standard way to deal with diminishing the responsive power is to utilize a compensator between the source and the load. Theoretical configurations of the compensator regularly expect that the identical source comprises of a perfect generator having zero output impedance and delivering an altered, simply sinusoidal voltage. On the off chance that the load is straight time invariant (LTI), the subsequent enduring state mutt rent is a stage moved sinusoid, and the PF is the cosine of the phase shift point. Accessible compensation innovations incorporate e.g. the pivoting hardware as well as exchanged capacitors and inductors and power electronic converters, for example, dynamic channels and adaptable air conditioning transmission frameworks.

4.2 Reactive Power Review

Energy handling frameworks have experienced significant changes as of late. This procedure is principally determined by a longing to build proficiency, with diminishment in energy costs, energy losses (and cooling necessities), and part measure. For productivity changes have been created the new advancements, (for example, power electronics), and use of quicker actuators and controllers.

It is imperative that there exist useful impediments applicable for displaying and control of dormant power. For instance, because of limited exchanging frequency there exists a scope of frequencies where a dynamic channel (regularly a voltage sourced inverter) can work viably. The execution criteria are themselves innovation subordinate—numerous instruments accessible in the field can just gauge amounts in the scope of roughly 1.5 kHz, however the most astounding harmonic utilized for metering reasons for existing is frequently the 23rd. Another for all intents and purposes essential class of requirements is powered by material science of voltage sourced inverters, for example, limited energy storage, with constrained permitted voltage variety of the primary capacitor and conceivably lacking voltage extent for following of higher current harmonics.

(a) Harmonic Standards: Standards and suggestions that recommend execution criteria for electrical hardware are advanced by various associations around the world (more than 50 national guidelines are said in [1]). The most powerful ones originate from the International Electrotechnical Commission (IEC) and by the IEEE, [1–3]. While the IEEE-519 prescribed practice concentrates on the client/framework interface (the purported purpose of regular coupling) and on higher power levels, the IEC-1000 standard (additionally embraced as the European standard) incorporates limits for individual bits of gear, and approaches to gauge the harmonic. These archives commonly list the extent of particular (low) current harmonics (both in relative and in outright terms), and an aggregate amount known as the total harmonic distortion (*THD*), that confines a potentially weighted total of squares of consonant sizes. Watch that all significant global measures are indicated in the frequency area. While these benchmarks can be deciphered as outside imperatives powered on the specialist outlining an energy handling framework, it is critical to recall the real framework indications of expanded harmonics. These incorporate hardware impacts, (for example, disappointments of wires, power component redress capacitors, transformer and engine overheating, breaker stumbling) and framework wide issues (squinting of glowing lights and glint of glaring lights, impedance on correspondence frameworks) [3]. A late study of North American utilities [4] recommended that while the quantity of loads that create current harmonic when supplied with a (near) sinusoidal voltage is expanding powerfully, there exists an essential absence of comprehension of energy streams including nonsinusoidal waveforms and of approaches to decipher benchmarks.

A word about classification while everybody concurs that dynamic (or genuine) power is the dc part of the prompt power (every one of these amounts will be characterized right away), a few creators save the name responsive power for the supplement of dynamic power (the dormant power) at major frequency, or for the component that can be repaid with direct latent circuit component; we utilize the assignments reactive and idle reciprocally (for additional on a proposed brought together phrasing see [5]).

(b) Power Systems: A spearheading chip away at this subject was attempted in Europe in the seventies, and brought about the Fryze-Buchholz-Depenbrock (FBD) strategy, compressed by the originator in [6]. This reference brings up the likelihood of figuring ideas in the frequency space. Late down to earth uses of this time-area approach are exhibited in [7, 8].

Different references by Czarnecki, e.g. [9–13] together with here and there warmed running with trade [14], tended to the issue from a power structure perspective, and portrayed diverse miracles of utilitarian energy for circuit-based compensation in unbalanced three-stage systems. A repeat space presentation of Czarnecki breaking down of three-stage systems is presented in [9]; we later give a complete explanation in the general case. Note that other orthogonal weakenings are doable for the sections of the inactive present, for instance, the one showed in

[15] that disconnects the part compensable by direct shunt components. A related responsibility by an IEEE Power-Engineering Society Working Group is shown in [16]. An instructive and sensible power system test is given in [17].

The unmistakable power is one of the key thoughts while describing diverse sums in polyphase structures, and a material science based comprehension is given in [18]; a former study on the subject is depicted in [19]. A novel power system organized presentation of the thought responsive power with respect to vector spaces and repeat parts is given in [20]. From the theoretical perspective, our investigation heading contrasts from the strategy depicted in [20] in our emphasis on projections in vector spaces where a polyphase sign is identified with by a singular part (point) of a suitable Hilbert space. This new vector space licenses us to decide a united treatment of each and every genuine class of responsive power compensators as projections to suitable sub-spaces, and structures a reason for fruitful numerical procedure.

(c) Power Electronics: The exploration on polyphase frameworks in nonsinusoidal operation has been reinvigorated by [21] that drew closer the issue from a down to earth stance, and proposed a helpful definition for the "quick" reactive power. (An undifferentiated from idea was presented before by Depenbrock as pointed out in [6], yet remained basically obscure outside Germany.) The idea was introduced in the time space, and in the exceptional instance of three-stage frameworks, so that the thought of vector (external) results of vectors could be utilized. An augmentation to four-conductor frameworks that can represent the zero-sequence components was presented in [22, 23]. Note that the momentary responsive power relates to the part of the inert power that can be repaid without energy stockpiling. A compensator construct only with respect to this idea won't just neglect to totally dispose of the idle power, yet might likewise bring extra harmonic [24] into the present waveform, as we show later. This is recognized by one of the originators of the quick responsive power idea in [25]. Hypothetical ideas proposed by Depenbrock and Akagi-Nabae have been broadly tried tentatively, for the most part in dynamic channel applications. Some illustrative studies are [26–31]. On account of three-stage three-conductor frameworks, it is some of the time gainful to express applicable amounts regarding space vectors. The change is clear, and a trial confirmation is introduced in [32].

4.3 Theoretical Background—Properties of Homogenous Operators

In this part the properties of homogenous operators are presented [33, 34]. They are important for next parts of this chapter.

For any given periodic signal $x(t)$ of period T the homogenous integral operator is defined as

$$\hat{x}(t) = \omega\left(\psi(t) - \overline{\psi}\right) = \frac{2\pi}{T}\left(\psi(t) - \overline{\psi}\right) \tag{4.1}$$

where integral of voltage $x(t)$ is

$$\psi(t) = \int_0^t x(\tau)d\tau \tag{4.2}$$

and the average value over period T is

$$\overline{\psi} = \int_0^T \psi(\tau)d\tau \tag{4.3}$$

Similarly, the homogenous differential operator is

$$\breve{x}(t) = \frac{1}{\omega}\frac{dx(t)}{dt} \tag{4.4}$$

Note that $\hat{x}$ and $\breve{x}$ are dimensionally homogenous to basic quantity x [33]. The internal product of two periodic variables $x(t)$ and $y(t)$ is defined as

$$\langle x, y\rangle = \frac{1}{T}\int_0^T x(t)y(t)dt \tag{4.5}$$

and norm of variable $x(t)$ (X is rms—root mean square) is

$$\|x\| = \sqrt{\langle x, x\rangle} = \sqrt{\frac{1}{T}\int_0^T x^2(t)dt} = X \tag{4.6}$$

The homogenous operators have following properties [from (4.7) to (4.17)]

$$\left\langle x, \hat{x}\right\rangle = \left\langle x, \breve{x}\right\rangle = 0 \tag{4.7}$$

$$\left\langle \hat{x}, \breve{x}\right\rangle = -\|x\|^2 \tag{4.8}$$

$$x = \breve{y} \Leftrightarrow \hat{x} = y \tag{4.9}$$

$$\left\langle \hat{x}, y \right\rangle = -\left\langle x, \hat{y} \right\rangle \tag{4.10}$$

$$\left\langle \breve{x}, y \right\rangle = -\left\langle x, \breve{y} \right\rangle \tag{4.11}$$

$$\left\langle \hat{x}, \breve{y} \right\rangle = \left\langle \breve{x}, \hat{y} \right\rangle = -\langle x, y \rangle \tag{4.12}$$

Moreover, if x and y are sinusoidal quantities with rms values respectively equal to X and Y and phase difference equal to φ, the following properties hold:

$$\|x\| = \left\|\hat{x}\right\| = \left\|\breve{x}\right\| = X \tag{4.13}$$

$$\hat{x} + \breve{x} = 0 \tag{4.14}$$

$$x^2 + \hat{x}^2 = x^2 + \breve{x}^2 = x^2 - \hat{x}\breve{x} = 2\|x\|^2 = 2X^2 \tag{4.15}$$

$$xy - \hat{x}\breve{y} = xy - \breve{x}\hat{y} = 2XY \cos \varphi \tag{4.16}$$

$$\hat{x}y - x\hat{y} = x\breve{y} - \breve{x}y = 2XY \sin \varphi \tag{4.17}$$

Moreover, expressing variable $x(t)$ by its Fourier series:

$$x(t) = \sum_{k=1}^{\infty} x_k(t) = \sum_{k=1}^{\infty} \sqrt{2} X_k \sin(k\omega t + \varphi_k) \tag{4.18}$$

For homogenous variables

$$\hat{x}(t) = \sum_{k=1}^{\infty} \hat{x}_k(t) = -\sum_{k=1}^{\infty} \sqrt{2} \frac{X_k}{k} \cos(k\omega t + \varphi_k) \tag{4.19}$$

$$\breve{x}(t) = \sum_{k=1}^{\infty} \breve{x}_k(t) = \sum_{k=1}^{\infty} \sqrt{2} k X_k \cos(k\omega t + \varphi_k) \tag{4.20}$$

4.4 Cyclodissipativity Approach

It will be reflected the typical energy transmission from an AC generator to a load. The voltage and current of the supplier are functions of time and are stand for the column vectors v_S, $i_S \in \Re^q$. The load is defined by a (conceivably nonlinear and time-varying) q–port system Σ [35, 36].

There are will the two following assumptions:

(**A1**) All the signs in the system are periodic with fundamental period T and fit into the space

$$L_2[0,T): \left\{ x:[0,T) \to \Re^q \middle| \|x\|^2 := \frac{1}{T}\int_0^T |x(\tau)|^2 d\tau < \infty \right\} \tag{4.21}$$

where $\|.\|$ *is named the RMS* value of b *and* $|.|$ *is the Euclidean standard.*

(**A2**) *The supplier is ideal, in the sense that* v_S *stays unaffected for all loads.*

Assumption (A1) captures the essentially rational method that the organism functions in a periodic, though not unavoidably sinusoidal, steady-state system. This is the case of the vast majority of applications of attention for the problem at hand [36].

Assumption (A2) is the similar to saying that the supplier has zero impedance and is defensible by the fact that most AC device function at a specified voltage, with the actual drained current being stated by the load [36].

The active power supplied by the source is defined as

$$P := \langle v_S, i_S \rangle = \frac{1}{T}\int_0^T v_S^T(t) i_S(t) dt \tag{4.22}$$

and $\langle . \rangle$ means the internal creation in $L_2[0, T)$. From (4.22) and the Cauchy-Schwarz inequality [36] is

$$P \le \|v_S\| \cdot \|i_S\| =: S \tag{4.23}$$

where is defined the apparent power S. From the inequality above we achieve that, under Assumption (2), S is the uppermost average power supplied to the load for all loads that have the identical rms current $\|i_S\|$. The characteristics holds if and only if v_S and i_S are collinear. If this is not the case $P < S$ and compensation schemes are presented to decrease this incongruity [36]. That is, to maximize the proportion P/S - that is called the PF. A typical compensation formation (which can be easily prolonged to n-phase system) is shown in Fig. 4.1 where, to preserve the rated

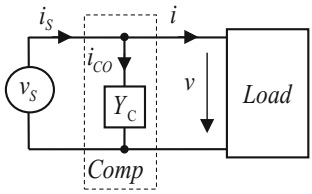

Fig. 4.1 Principle of typical reactive power compensation

voltage at the load stations the compensator Y_C is located in parallel. Similarly, to evade power indulgence, Y_C is restricted to be lossless, that is

$$\langle v, i_{CO} \rangle = 0 \tag{4.24}$$

where i_{CO} is the compensator current and notification that $v_S = v$ (Fig. 4.1). From the former can be result that the *PF* compensation problem is accurately equivalent to the problem of minimization of $\|i_S\|$ subject to the restriction (4.24). From

$$\|i_S\|^2 = \|i\|^2 + \|i_C\|^2 + 2\langle i_C, i \rangle \tag{4.25}$$

it is clear that an obligatory situation to decrease the rms value of i_S is

$$\langle i_C, i \rangle < 0 \tag{4.26}$$

It turns out that the latter circumstance and the limitation of compensator losslessness can be recognized using the perception of cyclo-dissipativity and its connected abstract energy [36–41].

Definition 1 Assume a dynamical system, with input $u \in L_2[0,T)$ and output $y \in L_2[0,T)$, acknowledges a state–space picture with state vector $x \in X$ [42]. The system is cyclo-dissipative with respect to the supply rate $w(u, y)$, where w: $L_2[0, T) \times L_2[0,T) \rightarrow \Re$, if and only if

$$\int_0^T w(u(t), y(t))dt \geq 0 \tag{4.27}$$

For all u: $[0, T) \rightarrow L_2[0,T)$ such that $x(T) = x_0$ where $x(0) = x_0$. It is said to be cyclo-lossless if the inequality holds with identity. *In other words, a system is cyclo-dissipative when it cannot create (abstract) energy over closed paths in the state-space.* It might, though, produce energy alongside some preliminary share of such a trajectory; if so, it would not be dissipative. *On the other hand, every dissipative system is cyclo-dissipative.* For instance, (possibly nonlinear) RLC circuits with input and output their terminal currents and voltages, respectively, are cyclo-dissipative with supply rate $w(u, y) = u^T y$ provided that all resistances are passive (This can be easily proven using Tellegen's Theorem [42–44]). Note that it is not presumed that inductors and capacitors are passive-that is, that their stored

energy is non–negative-if so, the circuit is in addition passive. It has been shown in [42–44] that, correspondingly to dissipative systems, one can use storage functions and dissipation differences to characterize cyclo-dissipativity.

Theorem 1 *A system with state depiction is cyclo-dissipative if, for all $x \in X$ which are both controllable and reachable, there exists a virtual storage function ϕ: $X \rightarrow R$ [42]. That is, a function that satisfies*

$$\phi(x_0) + \int_0^T w(u(t), y(t))dt \geq \phi(x_1) \tag{4.28}$$

for $u \in L_2[0,T)$ such that $x(0) = x_0$ and $x(T) = x_1$. In following part, the instances of reactive power compensation based on cyclo-dissipativity method are presented.

4.5 Reactive Power Compensation

In this part on the first, the simple example concerning linear circuit and nonharmonic power source is presented. The second example is devoted to nonlinear circuit. Booth examples are simply extended to q-phase version.

Example 4.1 [36]: Suppose linear system, power source, compensator and serial connection of *RLC* and nonharmonic power source (Fig. 4.2) [36]. Supply voltage v_S is

$$v_s(t) = \sqrt{2}(A_1 \sin(\omega_0 t) + A_3 \sin(3\omega_0 t) + A_5 \sin(5\omega_0 t)) \tag{4.29}$$

where $A_1 = 360$, $A_3 = 144$, $A_5 = 42$, $\omega_0 = 100\pi$ [rad/s] and $R = 15$ [Ω], $L = 0.08$ [H], $C = 0.0212$ [mF]. Load impedances Z_n (for $n = 1, 3, 5$) are given

$$Z_n = R + j\omega_0 nL + \frac{1}{j\omega_0 nC} \quad n = 1, 3, 5 \tag{4.30}$$

For calculated values $Z_1 = 15 - 125.14j$; $Z_3 = 15 + 24.97j$; and $Z_5 = 15 + 95j$, the effective currents are

$$i_n = A_n / Z_n \quad n = 1, 3, 5 \tag{4.31}$$

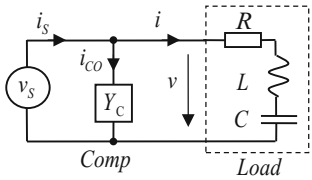

Fig. 4.2 Example of RP compensation for linear *RLC* load and nonharmonic source

Numerical values of currents are $i_1 = 0.34 + 2.8361j$; $i_3 = 2.54 - 4.24j$; $i_5 = 0.0681 - 0.4313j$.

Total effective current through the load is

$$i = \|i_n\| = \sqrt{\sum_n |i_n|^2} = \sqrt{|i_1|^2 + |i_3|^2 + |i_5|^2}; \quad n = 1, 3, 5 \tag{4.32}$$

therefore $i = 5.7257$ [A]. For *uncompensated circuit* ($Y_C \rightarrow 0$) $i_S = i$ and apparent power is

$$S = \|v_S\| \cdot \|i_S\| = \left(\sqrt{|A_1|^2 + |A_3|^2 + |A_5|^2}\right) \cdot \left(\sqrt{|i_1|^2 + |i_3|^2 + |i_5|^2}\right) \tag{4.33}$$

Result is $S = 2233$ [VA] and active power (average power) is

$$P = \langle v_S, i_S \rangle = \frac{1}{T} \int_0^T v_S^T(t) i_S(t) dt = R i_S^2 \tag{4.34}$$

$P = 491.8$ [W]. *PF* for uncompensated circuit ($Y_C \rightarrow 0$) is

$$PF = \frac{P}{S} = \frac{491.76}{2233} = 0.22 \tag{4.35}$$

For circuit compensated by capacitor

$$\|i_S\|^2 = \|i + i_{CO}\|^2 = \|i\|^2 + \|i_{CO}\|^2 + 2\langle i, i_{CO} \rangle \tag{4.36}$$

and current i_{C0} for compensation capacitor

$$i_{CO}(t) = C_{CO} \frac{dv_S(t)}{dt} \tag{4.37}$$

therefore

$$i_{CO} = C_{CO} \dot{v}_S \tag{4.38}$$

and substitution of Eq. (4.18) into (4.16)

$$\|i_S\|^2 = \|i + i_{CO}\|^2 = \|i\|^2 + \|C_{CO} \dot{v}_S\|^2 + 2\langle i, C_{CO} \dot{v}_S \rangle t \tag{4.39}$$

after some manipulations

$$\|i_S\|^2 = \|i + i_{CO}\|^2 = \|i\|^2 + C_{CO}^2\|\dot{v}_S\|^2 + 2C_{CO}\langle i, \dot{v}_S\rangle \tag{4.40}$$

For compensated circuit $\|i_S\|^2 < \|i + i_{CO}\|^2$ Eq. is

$$\|i_S\|^2 < \|i + i_{CO}\|^2 = \|i\|^2 + C_{CO}^2\|\dot{v}_S\|^2 + 2C_{CO}\langle i, \dot{v}_S\rangle \tag{4.41}$$

Using the property (4.42)

$$\langle \dot{x}, y\rangle = -\langle x, \dot{y}\rangle \tag{4.42}$$

in Eq. (4.41) results

$$\|i_S\|^2 < \|i + i_{CO}\|^2 = \|i\|^2 + C_{CO}^2\|\dot{v}_S\|^2 - 2C_{CO}\left\langle \dot{\hat{i}}, v_S\right\rangle \tag{4.43}$$

Minimal value of i_S (or minimum of apparent power S) can be found for

$$\frac{d}{dC_{CO}}\left(\|i\|^2 + C_{CO}^2\|\dot{v}_S\|^2 - 2C_{CO}\left\langle \dot{\hat{i}}, v_S\right\rangle\right) = 0 \tag{4.44}$$

therefore

$$2C_{CO}\|\dot{v}_S\|^2 - 2\left\langle \dot{\hat{i}}, v_S\right\rangle = 0 \tag{4.45}$$

Optimal value of compensation capacitor is

$$C_{CO} = \frac{\left\langle \dot{\hat{i}}, v_S\right\rangle}{\|\dot{v}_S\|^2} \tag{4.46}$$

where

$$\left\langle \dot{\hat{i}}, v_S\right\rangle = \mathrm{Re}\{j\omega_0 i_1 A_1\} + \mathrm{Re}\{j3\omega_0 i_3 A_3\} + \mathrm{Re}\{j5\omega_0 i_5 A_5\} = 282800 \tag{4.47}$$

and

$$\|\dot{v}_S\|^2 = (A_1\omega_0)^2 + (A_3 3\omega_0)^2 + (A_5 5\omega_0)^2 = 3.5563 \cdot 10^{10} \tag{4.48}$$

The optimal capacitor for compensation of reactive power [according (4.46)] is

$$C_{CO} = 282800/\left(3.5563 \cdot 10^{10}\right) = 7.9521[\mu\mathrm{F}]$$

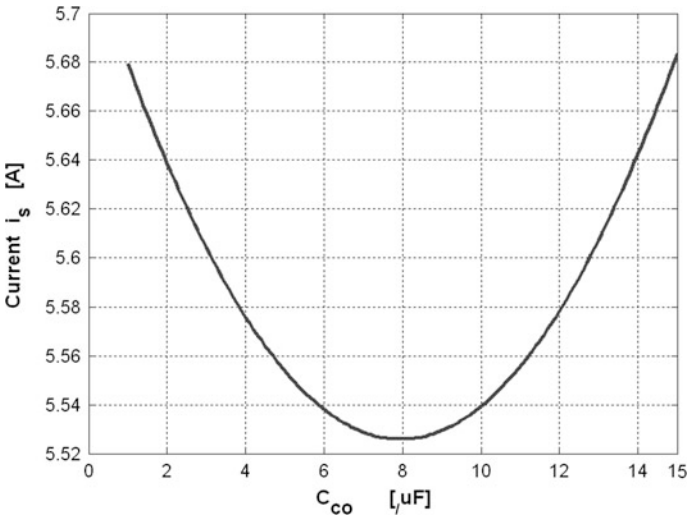

Fig. 4.3 Current i_S versus value of compensation capacitor C_{CO} (Example 4.1)

This result was confirmed by simulation (searching for optimal value) as Fig. 4.3. Currents through the compensation capacitor

$$i_{COn} = jn\omega_0 C_{CO} A_n;\ n = 1, 3, 5 \tag{4.49}$$

$i_{CO1} = 0 + 0.899j$; $i_{CO3} = 0 + 1.079j$; $i_{CO5} = 0 + 0.525j$ and currents from source after compensation $i_{S1} = 0.34 + 3.735j$; $i_{S3} = 2.545 - 3.158j$; $i_{S5} = 0.0681 + 0.0933j$, and total effective current from source for circuit with compensation capacitor is $i_S = 5.5259$ (without compensation was 5.72 A) and apparent power is $S = 2155$. PF for compensated circuit is $PF = P/S = 491.8/2155 = 0.228$.

The circuit can be compensated also by inductor where compensation current is given as

$$i_L = \frac{1}{L_C}\int v_S dt \tag{4.50}$$

For compensation by means of inductor, Eq. (4.43) is changed

$$\|i_S\|^2 < \|i + i_L\|^2 = \|i\|^2 + \left\|\frac{1}{L_C}\int v_S\right\|^2 + 2\left\langle \frac{1}{L_C}\int v_S, i\right\rangle \tag{4.51}$$

For compensated circuit

$$\|i_S\|^2 < \|i + i_L\|^2 = \|i\|^2 + \frac{1}{L_C^2}\left\|\int v_S\right\|^2 + \frac{2}{L_C}\left\langle i, \int v_S \right\rangle \tag{4.52}$$

After some manipulation, optimal value of compensation inductor is

$$L_C = \frac{-\left\|\int v_S\right\|^2}{\left\langle i, \int v_S \right\rangle} \tag{4.53}$$

where

$$\left\|\int v_S\right\|^2 = \left(\left|\frac{A_1}{\omega_0}\right|\right)^2 + \left(\left|\frac{A_3}{3\omega_0}\right|\right)^2 + \left(\left|\frac{A_5}{5\omega_0}\right|\right)^2 = 1.34 \tag{4.54}$$

and

$$\left\langle i, \int v_S \right\rangle = \mathrm{Re}\left\{j\frac{A_1}{\omega_0} i_1\right\} + \mathrm{Re}\left\{j\frac{A_3}{3\omega_0} i_3\right\} + \mathrm{Re}\left\{j\frac{A_5}{5\omega_0} i_5\right\} = -2.59 \tag{4.55}$$

Therefore optimal compensation inductor [according Eq. (4.53)] is

$$L_C = -1.337/-2.5909 = 0.516\ [\mathrm{H}] \tag{4.56}$$

This result was confirmed by simulation (Fig. 4.4). Current through the compensation inductor

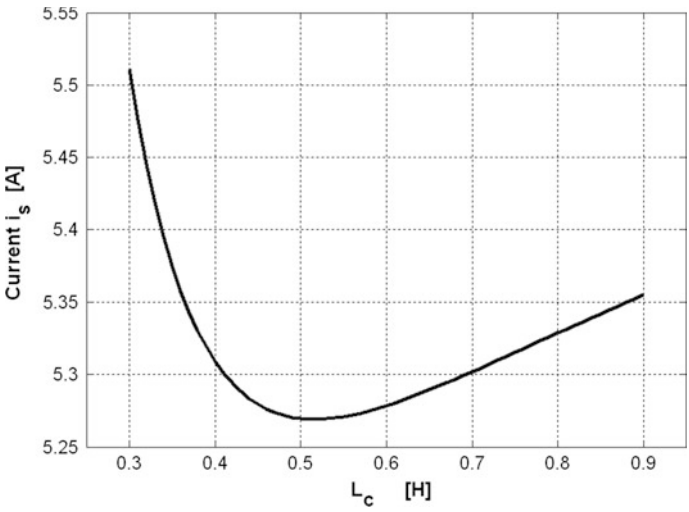

Fig. 4.4 Current i_S versus value of compensation inductor L_C (Example 4.1)

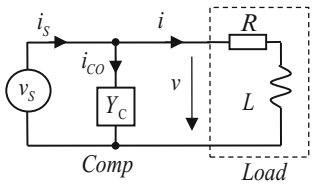

Fig. 4.5 Example of RP compensation for linear *RL* load and nonharmonic source

$$i_{Ln} = A_n/jn\omega_0 L_C; \quad n = 1, 3, 5\ldots \tag{4.57}$$

Calculated values are $i_{L1} = 0 - 2.22j$; $i_{L3} = 0 - 0.296j$; $i_{L5} = 0 - 0.052j$. Currents from source after compensation are $i_{S1} = 0.34 + 0.616j$; $i_{S3} = 2.545 - 4.534j$; $i_{S5} = 0.068 - 0.483j$ and total effective current from source for circuit with compensation inductor is $i_S = 5.27$, and apparent power is $S = 2055$, and PF for compensated circuit is $PF = P/S = 491.8/2055 = 0.24$.

This result was confirmed by simulation (searching for optimal value) as Fig. 4.4.

Example 4.2 [36]: Suppose linear system, power source, compensator and serial connection of *RL* and nonharmonic power source shown in Fig. 4.5 [36], instead of nonlinear inductor the nonharmonic power source is used. Supply voltage v_S is

$$v_s(t) = \sqrt{2}(A_1 \sin(\omega_0 t) + A_3 \sin(3\omega_0 t)) \tag{4.58}$$

where $A_1 = 220$, $A_3 = 70$, $\omega_0 = 100\pi$ [rad/s] and $R = 10$ [Ω], $L = 0.2$ [H]. Similarly as in Example 4.1, the load impedances Z_n (for $n = 1, 3$) are given

$$Z_n = R + j\omega_0 nL \quad n = 1, 3 \tag{4.59}$$

For calculated values $Z_1 = 10 + 62.8j$, $Z_2 = 10 + 188.5j$, the effective currents are $i_1 = 0.54 - 3.4j$; $i_3 = 0.02 - 0.37$j;

For *uncompensated circuit* ($Y_C \to 0$), total effective current through the load according Eq. (4.22) is $i_S = i = 3.48$ [A] and apparent power (4.23) is $S = 802.9$ [VA] and active power (4.24) is $P = 121$ [W]. For uncompensated circuit is $PF = 0.15$. By the same way as in previous Example 4.1, using (4.40), (4.45) and (4.46) calculated values are

$$\left\langle \dot{\hat{i}}, v_S \right\rangle = 260450 \tag{4.60}$$

and

$$\|\dot{v}_S\|^2 = 9.13 \cdot 10^9 \tag{4.61}$$

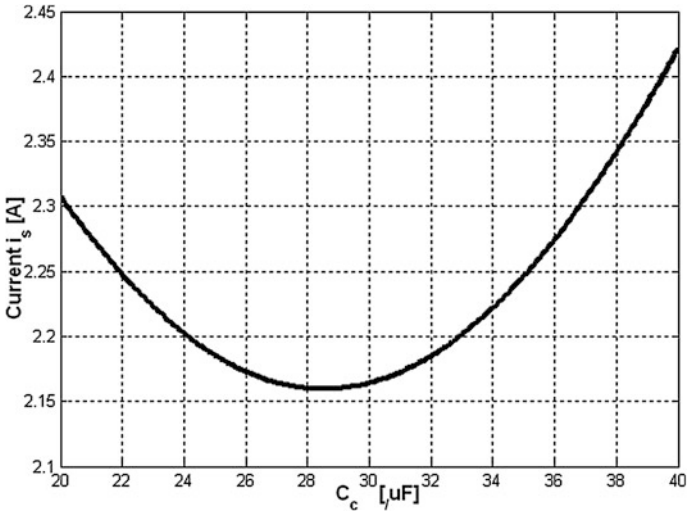

Fig. 4.6 Current i_S versus value of compensation capacitor C_{CO} (Example 4.2)

Optimal value of compensation capacitor is

$$C_{CO} = \frac{\left\langle \dot{\hat{i}}, v_S \right\rangle}{\|\dot{v}_S\|^2} = \frac{260450}{9.13 \cdot 10^9} = 28.5 \cdot 10^{-6} \tag{4.62}$$

This result was confirmed by simulation (searching for optimal value) as Fig. 4.6.

For circuit compensated by capacitor $i = 2.16$ [A] and apparent power is $S = 498.6$ [VA], active power is $P = 121$ [W] and. $PF = 0.22$. The compensation by means of inductor is not possible because result according Eq. (4.53) has negative sign. Simulation results are shown in Fig. 4.7, where compensation capacitor is connected in time ≥ 0.44 s.

Example 4.3 [36]: Suppose nonlinear circuit with triac (Fig. 4.8) and non-sinusoidal power source $v_S(t) = 220\sin(100\pi t) + 30\sin(300\pi t)$, $R = 10\ \Omega$ and $\alpha = \pi/2$. By the same way as in previous Example 4.1, using (4.60), (4.61) and (4.62) calculated values are

$$\left\langle \dot{\hat{i}}, v_S \right\rangle = -\langle i, \dot{v}_S \rangle = -3.6 \cdot 10^5 \tag{4.63}$$

and

$$\|\dot{v}_S\|^2 = 5.58 \cdot 10^9 \tag{4.64}$$

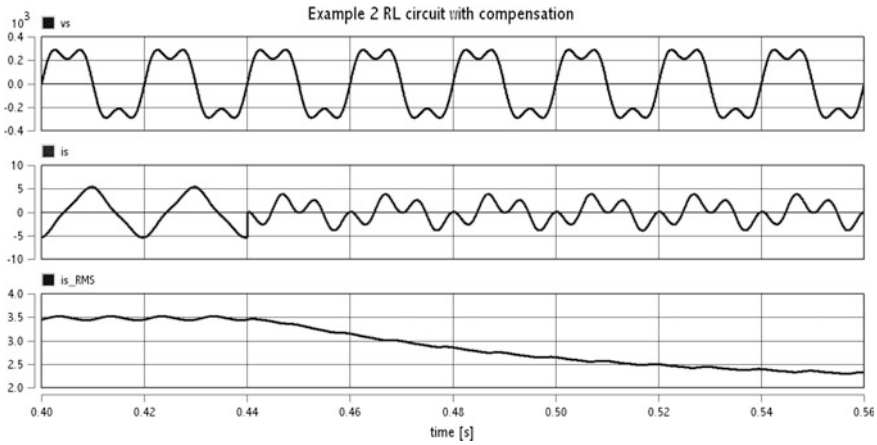

Fig. 4.7 Time evolution of voltage (*top*), current from source (*middle*) and effective current from source for uncompensated (time <0.44) and compensated circuit (time ≥ 0.44)

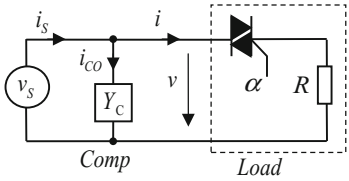

Fig. 4.8 Nonlinear circuit with triac

Optimal value of compensation capacitor can be calculated from

$$C_{CO} = \frac{-\langle i, \dot{v}_S \rangle}{\|\dot{v}_S\|^2} = \frac{-(-3.6 \cdot 10^5)}{5.58 \cdot 10^9} = 64.7 \cdot 10^{-6} \tag{4.65}$$

Optimal value of compensation capacitor (C_{CO} = 65 [μF]) was confirmed by simulation as Fig. 4.9. For uncompensated circuit effective current is

$$i_S = 15.7\,[\mathrm{A}],\ P = 2462[\mathrm{W}],\ S = 3484\,[\mathrm{VA}],\ PF = 0.71$$

After compensation effective current from source is

$$i_S = 14.92\,[\mathrm{A}],\ P = 2462\,[\mathrm{W}],\ S = 3315\,[\mathrm{VA}],\ PF = 0.743$$

The time evolutions of signals in nonlinear circuit are shown in Fig. 4.10. It is important to note that inductor is not possible for compensation because result according Eq. (4.53) has negative sign.

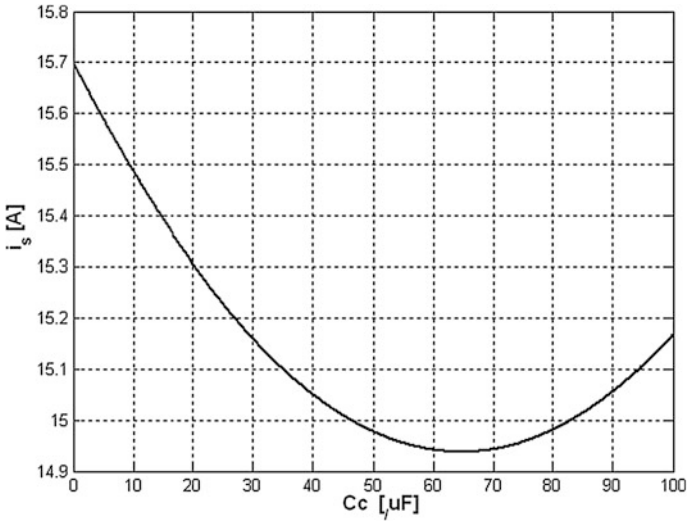

Fig. 4.9 Current i_S versus value of compensation capacitor C_{CO} for nonlinear circuit (Example 4.3)

Previous results can be used for automatic compensation of RP. The time evolution of signals (for circuit in Fig. 4.8) is shown in Fig. 4.11. In time of $t_1 = 0.2$ [s] start automatic compensation [repeated evaluation of Eq. (4.64)] and changing value of compensation capacitor according condition in circuit ($C_{CO} = f(i_S(t),v_S(t))$).

From the beginning, until t_2 the power source voltage is $v_S(t) = 220\ \sin(100\pi t) + 30\ \sin(300\pi t)$ after t_2 voltage is sinusoidal $v_S(t) = 220\ \sin\ (100\pi t)$.

The effective value of supply current i_i is repeatedly calculated and smoothed by low-pass filter. From the Fig. 4.11 can be seen decreasing supply current value after start of compensation and once more decreasing after changing supply voltage to pure sinusoidal. In Fig. 4.12, the Value of compensation capacitor versus triac fire angle alpha is displayed.

4.6 Extension to Three-Phase Networks

The recently proposed networks were devoted to the analysis of single phase systems. In this chapter it is extended to three-phase networks.

The extension of the above theory to poly-phase systems is straightforward for 4 wire Y connection, but for 3 wire network with unbalanced terms, delta connection and compensation of reactive power opens several questions [45–47]. In this part the compensation of reactive power and unbalanced currents of three-phase network will described [48–52].

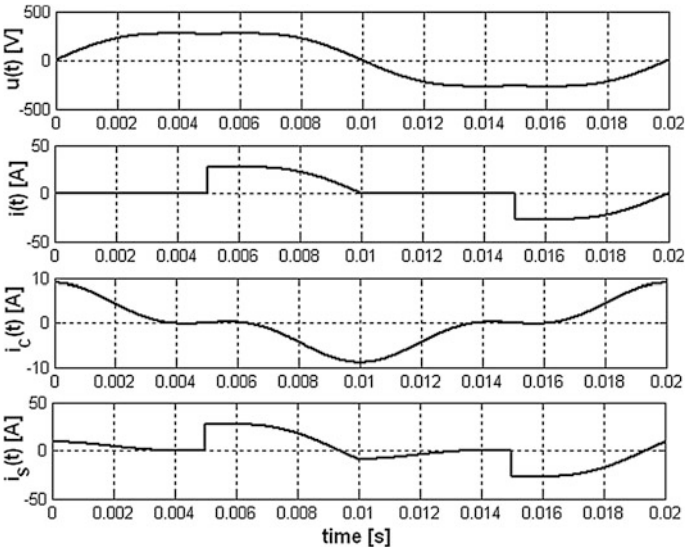

Fig. 4.10 Voltage and currents in nonlinear circuit. From *top* to *bottom*: Power source voltage, current through the load, current through compensation capacitor and current from source after compensation (Example 4.3)

Considerations in this part are devoted to three-phase, three-wire circuits, shown in Fig. 4.13 with linear, time-invariant loads supplied with a sinusoidal symmetrical voltage [53–55]. For any such loads there exist equivalent resistive and balanced loads shown in Fig. 4.14 that at the same voltage has the same active power P, as the original load. The Three-phase source with line resistance, transformer TR (Δ to Y connection) and load Z_R, Z_S, Z_T is shown in Figs. 4.15 (without compensation) and 4.16 (with compensation).

Suppose three-phase, sinusoidal line-to-ground voltages u_R, u_S and u_T and line currents i_R, i_S and i_T. The active and reactive powers is defined as

$$P = \frac{1}{T}\int_0^T (u_R i_R + u_S i_S + u_T i_T)dt = \sum_{f=R,S,T} U_f I_f \cos(\varphi_f) \tag{4.66}$$

$$Q = \sum_{f=R,S,T} U_f I_f \sin(\varphi_f) \tag{4.67}$$

There are several definitions of apparent power S. The definition according (4.68) is used

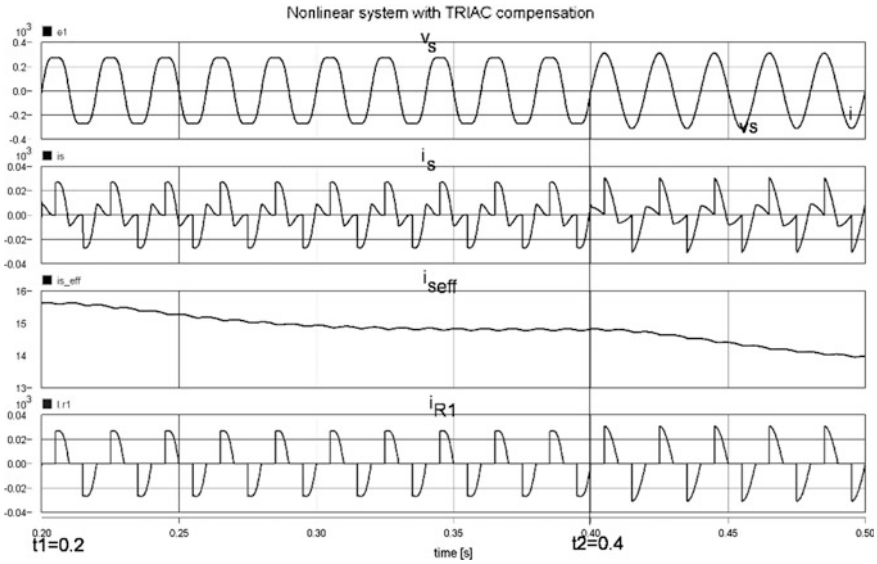

Fig. 4.11 Time diagram of voltage and currents in nonlinear circuit during the automatic compensation. From *top* to *bottom*: Voltage of power source, supply current i_S, effective value of supply current, current through the load. Compensation start in time $t = 0.2$. Source voltage is changed in $t = 0.4$ to pure sinusoidal. The time slice is $\langle 0.20 \div 0.50 \rangle$ (Example 4.3)

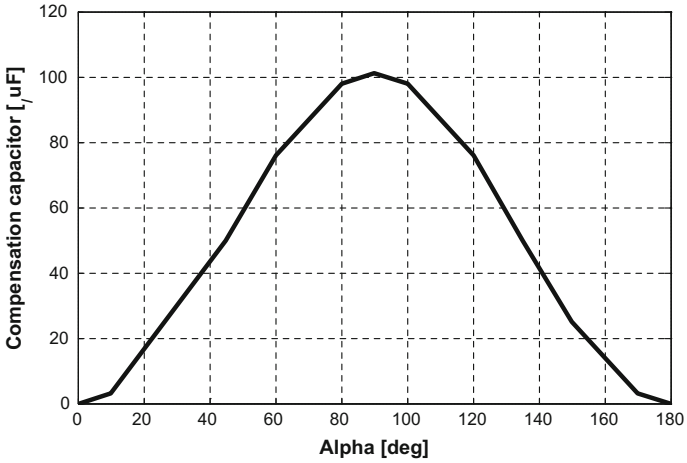

Fig. 4.12 Value of compensation capacitor versus alpha (Example 4.3)

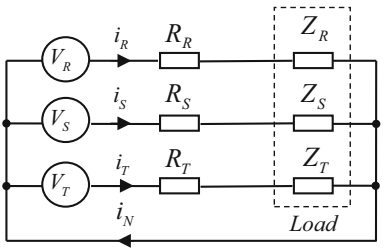

Fig. 4.13 Three-phase star (Y) network with line resistances R_R, R_S, R_T, loads Z_R, Z_S, Z_T and neutral wire

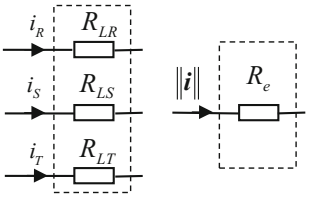

Fig. 4.14 Three-phase resistive load R_{LR}, R_{LS}, R_{LT} and its equivalent R_e

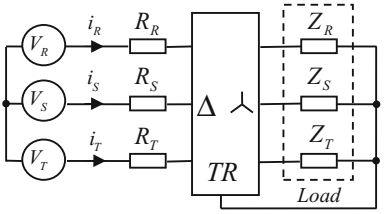

Fig. 4.15 Three-phase source with line resistance, transformer *TR* (Δ to Y) and load Z_R, Z_S, Z_T

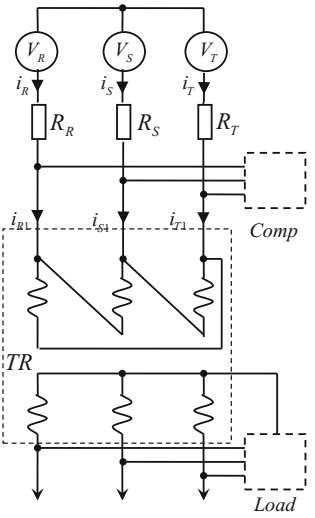

Fig. 4.16 Three-phase network with transformer *TR* (Δ to Y connection), load and compensation

$$S = \sqrt{U_R^2 + U_S^2 + U_T^2} \cdot \sqrt{I_R^2 + I_S^2 + I_T^2} = \|u\| \cdot \|i\| \tag{4.68}$$

The active power in three-phase system in frequency domain is

$$P = (u, i) = \mathrm{Re} \sum_{n \in N} U_n^T I_n^* \tag{4.69}$$

where asterisk denotes a conjugate number. The RMS value of a three-phase vector is defined as:

$$\|x\| = \sqrt{\sum_{n \in N} X_n^T \cdot X_n^*} = \sqrt{\sum_{n \in N} [X_{Rn}, X_{Sn}, X_{Tn}] \begin{bmatrix} X_{Rn}^* \\ X_{Sn}^* \\ X_{Tn}^* \end{bmatrix}} \tag{4.70}$$

For serial connection of R_Z and L_Z between phase R-S admittance is

$$Y_{RS} = \frac{1}{R_Z + j\omega L_Z} = \frac{1}{R_Z + X_Z} \tag{4.71}$$

The equivalent admittance Y_e for three admittances is

$$Y_e = Y_{RS} + Y_{ST} + Y_{TR} \tag{4.72}$$

The equivalent admittance G_e and susceptance B_e are given by

$$G_e = \mathrm{Re}(Y_e); \quad B_e = \mathrm{Im}(Y_e) \tag{4.73}$$

Unbalanced admittance A is

$$A = -(Y_{ST} + Y_{TR} e^{j2\pi/3} + Y_{RS} e^{j4\pi/3}) \tag{4.74}$$

Voltage v across phase is

$$v = \sqrt{3} v_f \tag{4.75}$$

Active current i_a, reactive current i_r unbalanced current i_u and total current i are

$$\begin{aligned} &i_a = G_e v = G_e \sqrt{3} v_f;\ i_r = |B_e| v;\ i_u = |A \cdot v| \\ &\|i\| = \sqrt{\|i_a\|^2 + \|i_r\|^2 + \|i_u\|^2} \end{aligned} \tag{4.76}$$

Active power P

$$P = G_e v_s^2 = G_e \|v\|^2 \tag{4.77}$$

Reactive power Q

$$Q = \|v\| \cdot \|i_r\| = -\mathrm{Im}\left\{ Y_{RS}\|u_{RS}\|^2 + Y_{ST}\|u_{RS}\|^2 + Y_{TR}\|u_{RS}\|^2 \right\} = -B_e\|v\|^2 \tag{4.78}$$

Unbalanced power D

$$D = \|v\| \cdot \|i_u\| = |A|\|v\|^2 \tag{4.79}$$

Apparent power S is calculated by

$$S = \|v\| \cdot \|i\| = \sqrt{P^2 + Q^2 + D^2} \tag{4.80}$$

Power Eq. (4.80) shows that reactive power and unbalanced power (reactive current and unbalanced current) increase apparent power and decrease power factor [Eq. (4.35)]. Thus reduction of booth currents leads to PF improvement. These currents can be reduced by shunt compensator. Compensator is composed from reactive passive parts e.g. inductors and capacitors, or three-phase inverter with control systems. The structure of reactive compensator is shown in Fig. 4.18 (*Comp*), susceptances W_{RS}, W_{ST} and W_{TR}, connected in delta configuration (it is supposed that W_{RS}, W_{ST} and W_{TR} are ideal loss-less parts).

From unbalanced admittance A and equivalent susceptance B_e is possible calculate the compensation susceptances W_{XY} from following equations. The reactive current is compensated if:

$$B_e + W_{RS} + W_{ST} + W_{TR} = 0 \tag{4.81}$$

The unbalanced current is compensated if

$$\begin{aligned} &A - j\left(W_{ST} + e^{j2\pi/2}W_{TR} + e^{j4\pi/2}W_{RS}\right) = 0 + j0 \\ &A - j\left(W_{ST} + \left(-\frac{1}{2} + j\frac{\sqrt{3}}{2}\right)W_{TR} + \left(-\frac{1}{2} - j\frac{\sqrt{3}}{2}\right)W_{RS}\right) = 0 + j0 \end{aligned} \tag{4.82}$$

The Eq. (4.82) is split on real and imaginary parts. Real part:

$$\mathrm{Re}\left\{A - j\left(W_{ST} + \left(-\frac{1}{2} + j\frac{\sqrt{3}}{2}\right)W_{TR} + \left(-\frac{1}{2} - j\frac{\sqrt{3}}{2}\right)W_{RS}\right)\right\} = 0 \tag{4.83}$$

Imaginary part:

$$\mathrm{Im}\left\{A - j\left(W_{ST} + \left(-\frac{1}{2} + j\frac{\sqrt{3}}{2}\right)W_{TR} + \left(-\frac{1}{2} - j\frac{\sqrt{3}}{2}\right)W_{RS}\right)\right\} = 0 \tag{4.84}$$

Therefore real part

$$\mathrm{Re}\{A\} = \frac{\sqrt{3}}{2}W_{RS} - \frac{\sqrt{3}}{2}W_{TR} \tag{4.85}$$

Imaginary part

$$\mathrm{Im}\{A\} = -\frac{1}{2}W_{RS} - \frac{1}{2}W_{TR} + W_{ST} \tag{4.86}$$

Add Eqs. (4.86) and (4.81) multiplied by −1

$$\left.\begin{aligned}\mathrm{Im}\{A\} &= -\tfrac{1}{2}W_{RS} - \tfrac{1}{2}W_{TR} + W_{ST}\\ B_e &= -W_{RS} - W_{TR} - W_{ST}\end{aligned}\right\} + \tag{4.87}$$

Result is

$$\mathrm{Im}\{A\} + B_e = -\frac{3}{2}W_{RS} - \frac{3}{2}W_{TR} \tag{4.88}$$

Now add Eqs. (4.88) and (4.85) multiplied by $\sqrt{3}$

$$\left.\begin{aligned}\mathrm{Im}\{A\} + B_e &= -\tfrac{3}{2}W_{RS} - \tfrac{3}{2}W_{TR}\\ \sqrt{3}\mathrm{Re}\{A\} &= \tfrac{3}{2}W_{RS} - \tfrac{3}{2}W_{TR}\end{aligned}\right\} + \tag{4.89}$$

Result is

$$\sqrt{3}\mathrm{Re}\{A\} + \mathrm{Im}\{A\} + B_e = -3W_{TR} \tag{4.90}$$

After manipulation

$$W_{TR} = \left[-\sqrt{3}\cdot\mathrm{Re}(A) - \mathrm{Im}(A) - B_e\right]/3 \tag{4.91}$$

and also

$$W_{RS} = \left[\sqrt{3}\mathrm{Re}(A) - \mathrm{Im}(A) - B_e\right]/3 \tag{4.92}$$

$$W_{ST} = [2\cdot\mathrm{Im}(A) - B_e]/3 \tag{4.93}$$

Values of compensation capacitors C_{XY} or inductors L_{XY} are calculated by

$$\text{if}\begin{cases} W_{XY} > 0 & \text{then} \quad C_{XY} = \frac{W_{XY}}{\omega} \\ W_{XY} < 0 & \text{then} \quad L_{XY} = -\frac{1}{\omega W_{XY}} \end{cases} \tag{4.94}$$

The previous derivation and results will used in next two examples for three-phase network compensation.

Example 4.4 [50, 51]: Suppose three-phase network with loss-less transformer *TR* (1:1) in Δ−Y connection and non-symmetrical resistive load $Z_L = R_L = 3\ \Omega$, $V_R = 277\angle 0°$, $V_S = 277\angle 120°$, $V_T = 277\angle 240°$ V, $\omega = 2\pi f = 314$, $R_R = R_S = R_T = 0.01\ \Omega$ (Figs. 4.17, 4.18, 4.19 and 4.20).

$$Y_{RS} = \frac{1}{R_Z + j\omega L_Z} = \frac{1}{R_Z + X_Z} = \frac{1}{3 + j0} \tag{4.95}$$

The equivalent admittance Y_e is

$$Y_e = Y_{RS} + Y_{ST} + Y_{TR} = \frac{1}{3 + j0} + 0 + 0 = 0.33 \tag{4.96}$$

The equivalent admittance G_e and susceptance B_e are given by

$$G_e = \text{Re}(Y_e) = \text{Re}(Y_{RS}) = 0.33; \quad B_e = \text{Im}(Y_e) = \text{Im}(Y_{RS}) = 0 \tag{4.97}$$

Unbalanced admittance A is

$$A = -(Y_{ST} + Y_{TR}e^{j2\pi/3} + Y_{RS}e^{j4\pi/3}) = -(0.33e^{j4\pi/3}) = 0.167 + 0.289j \tag{4.98}$$

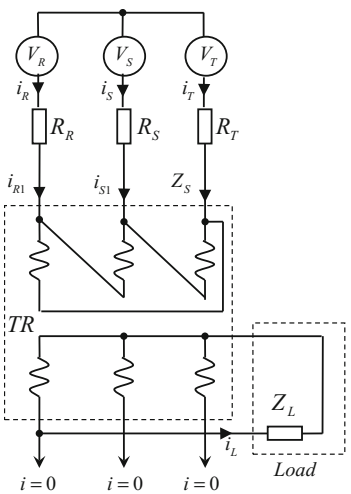

Fig. 4.17 Three-phase network with transformer *TR* (Δ to Y connection) with unbalanced load

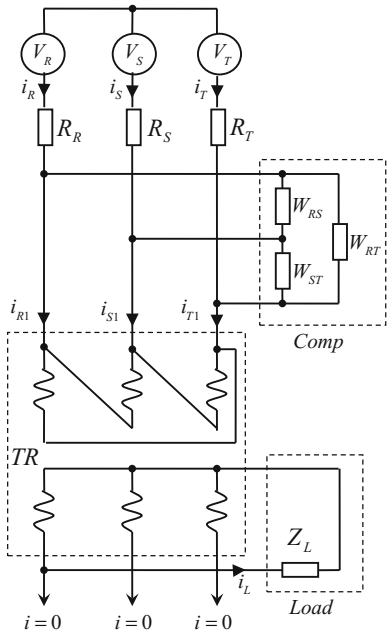

Fig. 4.18 Three-phase network with transformer *TR* (Δ to Y connection) with unbalanced load and compensation circuit

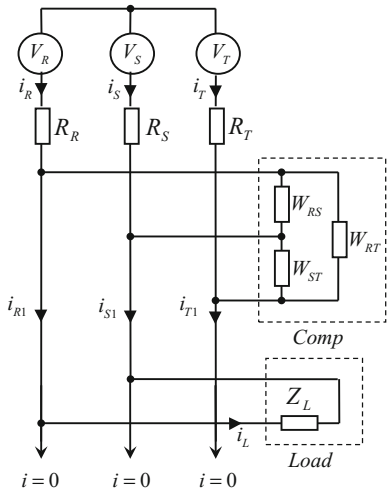

Fig. 4.19 Three-phase equivalent network with unbalanced load and compensation circuit. Avoid of transformer (Figs. 4.17 and 4.18) was possible by means of Y-load to Δ-load transformation

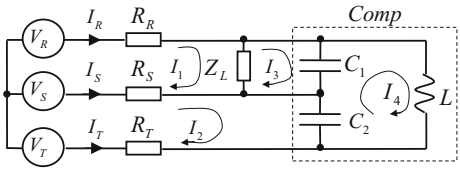

Fig. 4.20 Three-phase network with load Z_L and compensation parts C_1, C_2 and L

Voltage across phase v is

$$v = \sqrt{3}v_f = \sqrt{3} \cdot 277 = 480 \tag{4.99}$$

Active current i_a, reactive current i_r unbalanced current i_u and total current i are

$$\begin{aligned} &i_a = G_e v = G_e\sqrt{3}v_f = 160;\ i_r = |B_e|v = 0;\ i_u = |A \cdot v| = 160 \\ &\|i\| = \sqrt{\|i_a\|^2 + \|i_r\|^2 + \|i_u\|^2} = \sqrt{160^2 + 0 + 160^2} = 226 \end{aligned} \tag{4.100}$$

Active power

$$P = G_e v_s^2 = G_e \|v\|^2 = 76729 \tag{4.101}$$

Reactive power Q

$$Q = -\mathrm{Im}\left\{ Y_{RS}\|u_{RS}\|^2 + Y_{ST}\|u_{RS}\|^2 + Y_{TR}\|u_{RS}\|^2 \right\} = -B_e v_s^2 = -B_e\|v\|^2 = 0 \tag{4.102}$$

Unbalanced power D

$$D = \|v\| \cdot \|i_u\| = |A|\|v\|^2 = 479.7 \cdot 160 = 76.7 \cdot 10^3 \tag{4.103}$$

Phase currents for uncompensated circuit $i_R = i_S = 160$ A, $i_T = 0$. Apparent power S and power factor PF for uncompensated circuit

$$S = \|v\| \cdot \|i\| = 479.7 \cdot 226 = 1.1 \cdot 10^5;\ PF = \frac{P}{S} = \frac{76729}{110000} = 0.7 \tag{4.104}$$

From unbalanced admittance A and equivalent susceptance B_e is possible calculate the compensation susceptances W_{xy} according following equations

$$W_{RS} = \left[\sqrt{3}\mathrm{Re}(A) - \mathrm{Im}(A) - B_e\right]/3 = \frac{0.289 - 0.289}{3} = 0 \tag{4.105}$$

$$W_{ST} = [2 \cdot \mathrm{Im}(A) - B_e]/3 = \frac{2 \cdot 0.289 - 0}{3} = 0.192 \tag{4.106}$$

$$W_{TR} = \left[-\sqrt{3} \cdot \mathrm{Re}(A) - \mathrm{Im}(A) - B_e\right]/3 = \frac{-0.289 - 0.289 - 0}{3} = 0.192 \tag{4.107}$$

Values of compensation capacitors and inductors are calculated according Eq. (4.84)

$$\begin{aligned} C_1 &= \frac{W_{RS}}{\omega} = \frac{0}{314} = 0 \\ C_2 &= \frac{W_{ST}}{\omega} = \frac{0.192}{314} = 6.13 \cdot 10^{-4} \\ L &= -\frac{1}{\omega W_{TR}} = -\frac{1}{314 \cdot (-0.192)} = 0.016 \end{aligned} \tag{4.108}$$

Phase currents for compensated circuit $\|i_R| = \|i_S| = \|i_T| = 92.4$ A. Apparent power S and power factor PF for compensated circuit is

$$S = \|v\| \cdot \|i\| = 479.7 \cdot \sqrt{3 \cdot 92.4^2} = 7.9 \cdot 10^3;\ PF = \frac{P}{S} = \frac{76700}{79000} = 0.97 \tag{4.109}$$

The circuit diagram for network with compensation is shown in Fig. 4.20. Solving the Eqs. (4.85)–(4.89) gives the same results (phase currents) as previous calculation.

$$\begin{aligned} &R_R I_1 + Z_L(I_1 - I_3) + R_S(I_1 - I_2) = U_R \angle 0 - U_S \angle -120 \\ &R_S(I_2 - I_1) - \frac{j}{\omega C_2}(I_2 - I_4) + R_T I_2 = U_S \angle -120 - U_T \angle 120 \\ &Z_L(I_3 - I_1) - \frac{j}{\omega C_1}(I_3 - I_4) = 0 \\ &j\omega L I_4 - \frac{j}{\omega C_2}(I_4 - I_2) - \frac{j}{\omega C_1}(I_4 - I_3) = 0 \end{aligned} \tag{4.110}$$

Matrix M derived from (4.110) is

$$M = \begin{bmatrix} R_R + R_S + Z_L & -R_S & -Z_L & 0 \\ -R_S & R_S + R_T + \frac{-j}{\omega C_2} & 0 & \frac{j}{\omega C_2} \\ -Z_L & 0 & Z_L + \frac{-j}{\omega C_1} & \frac{j}{\omega C_1} \\ 0 & \frac{j}{\omega C_2} & \frac{j}{\omega C_1} & j\omega L + \frac{-j}{\omega C_1} + \frac{-j}{\omega C_2} \end{bmatrix} \tag{4.111}$$

Matrix equation is

$$M \cdot \begin{bmatrix} I_1 \\ I_2 \\ I_3 \\ I_4 \end{bmatrix} = \begin{bmatrix} U_R \angle 0 - U_S \angle -120 \\ U_S \angle -120 - U_T \angle 120 \\ 0 \\ 0 \end{bmatrix} \tag{4.112}$$

Currents I_1 to I_4 can are calculated from

$$\begin{bmatrix} I_1 \\ I_2 \\ I_3 \\ I_4 \end{bmatrix} = M^{-1} \begin{bmatrix} U_R\angle 0 - U_S\angle -120 \\ U_S\angle -120 - U_T\angle 120 \\ 0 \\ 0 \end{bmatrix} \tag{4.113}$$

Phase currents are

$$I_R = I_1;\ I_S = I_2 - I_1;\ I_T = -I_2 \tag{4.114}$$

The theoretical derivations were supported by simulation. The network was simulated without compensation part and with compensation part, connected by switch SW (Fig. 4.21). The time evolution of V_R, I_R, V_S, I_S and V_T, I_T before compensation is shown in Fig. 4.22. The same time evolution of phase's voltages and currents after compensation is shown in Fig. 4.23. The Fig. 4.24 presents time evolution of effective values of phase currents before and after connection of compensation circuit (compensation circuit was connected in time = 0.44 s)

Example 4.5 [50, 51]: Suppose three-phase network with loss-less transformer *TR* (1:1) in Δ–Y connection and non-symmetrical *RL* load $Z_L = R_L + j\omega L_Z = 30 + j10$, $V_R = 6000 \angle 0°$, $V_S = 6000 \angle 120°$, $V_T = 6000 \angle 240°$ V, $\omega = 2\pi f = 314$ [rad/sec], $R_R = R_S = R_T = 0.1\ \Omega$ (Fig. 4.17).

$$Y_{RS} = \frac{1}{R_Z + j\omega L_Z} = \frac{1}{R_Z + X_Z} = \frac{1}{30 + j10} = 0.03 - 0.01j \tag{4.115}$$

The equivalent admittance Y_e is

$$Y_e = Y_{RS} + Y_{ST} + Y_{TR} = 0.03 - 0.01j \tag{4.116}$$

The equivalent admittance G_e and susceptance B_e are given by

$$G_e = \mathrm{Re}(Y_e) = \mathrm{Re}(Y_{RS}) = 0.03;\ B_e = \mathrm{Im}(Y_e) = \mathrm{Im}(Y_{RS}) = -0.01 \tag{4.117}$$

Unbalanced admittance A is

$$A = -(Y_{ST} + Y_{TR}e^{j2\pi/3} + Y_{RS}e^{j4\pi/3}) = 0.0237 + 0.021j \tag{4.118}$$

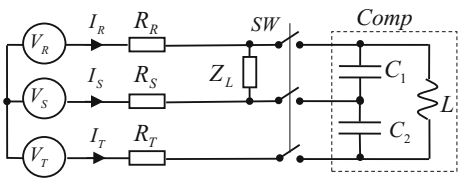

Fig. 4.21 Three-phase network with load Z_L, compensation parts C_1, C_2 and L and switch *SW* which is used for connection compensation parts

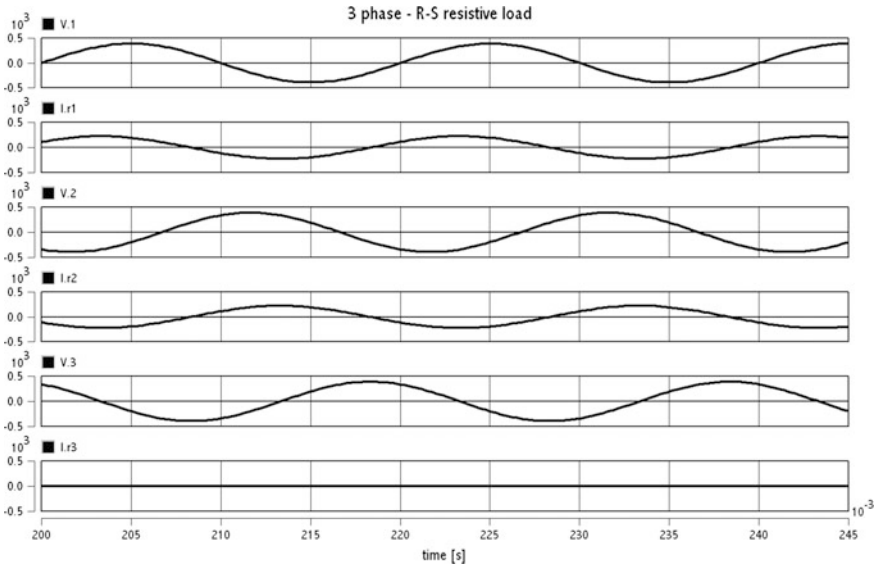

Fig. 4.22 Time evolution of voltages and currents in circuit according Example 4.4, before compensation. From *top* to *bottom*: Voltage V_R, current i_R, voltage V_S, current i_S, voltage V_T, current i_T

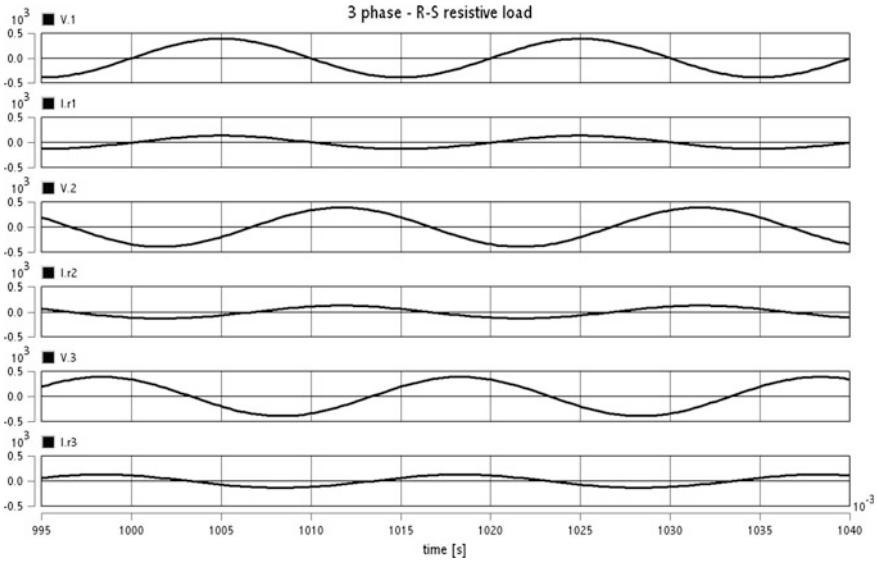

Fig. 4.23 Time evolution of voltages and currents in circuit according Example 4.4, after compensation. From *top* to *bottom*: Voltage V_R, current i_R, voltage V_S, current i_S, voltage V_T, current i_T

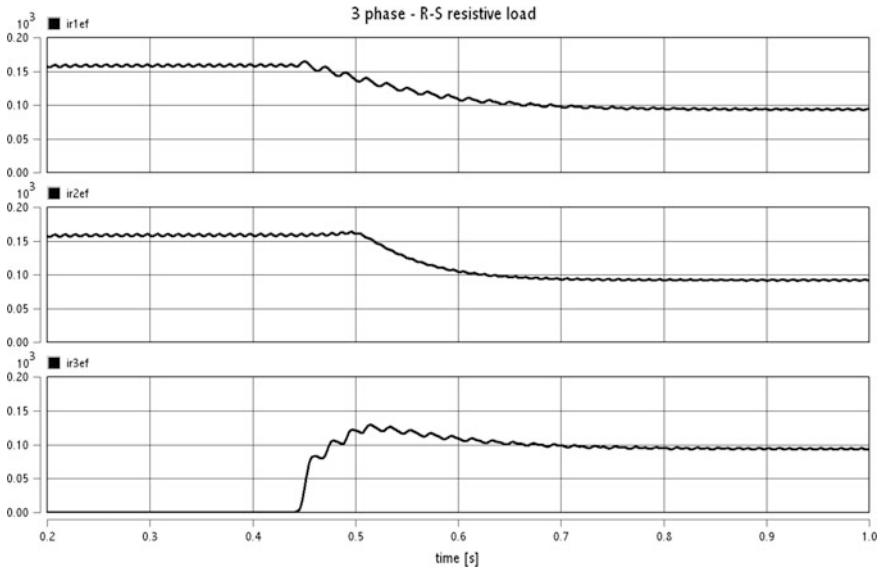

Fig. 4.24 Time evolution of RMS currents in circuit according Example 4.4, before and after compensation. Compensation parts are connected in time ≥ 0.44. From *top* to *bottom*: RMS currents i_R, i_S, i_T

Active current i_a, reactive current i_r unbalanced current i_u and total current i are

$$\begin{aligned} &i_a = G_e v = G_e\sqrt{3}v_f = 311.8;\ i_r = |B_e|v = 104;\ i_u = |A \cdot v| = 328.6 \\ &\|i\| = \sqrt{\|i_a\|^2 + \|i_r\|^2 + \|i_u\|^2} = 464.7 \end{aligned} \tag{4.119}$$

Active power

$$P = G_e v_s^2 = G_e \|v\|^2 = 3.24 \cdot 10^6 \tag{4.120}$$

Reactive power Q

$$Q = -B_e v_s^2 = -B_e \|v\|^2 = 1.08 \cdot 10^6 \tag{4.121}$$

Unbalanced power D

$$D = \|v\| \cdot \|i_u\| = |A|\|v\|^2 = 10392 \cdot 328.6 = 3.4 \cdot 10^6 \tag{4.122}$$

Phase currents for uncompensated circuit $i_R = i_S = 328.6$ A, $i_T = 0$. Apparent power S and power factor PF for uncompensated circuit

$$S = \|v\| \cdot \|i\| = 10392 \cdot 464.7 = 4.83 \cdot 10^6;\ PF = \frac{P}{S} = \frac{3.24 \cdot 10^6}{4.83 \cdot 10^6} = 0.67 \tag{4.123}$$

From unbalanced admittance A and equivalent susceptance B_e is possible calculate the compensation susceptances W_{xy} according following equations:

$$W_{RS} = \left[\sqrt{3}\mathrm{Re}(A) - \mathrm{Im}(A) - B_e\right]/3 = 0.01 \tag{4.124}$$

$$W_{ST} = [2 \cdot \mathrm{Im}(A) - B_e]/3 = 0.0173 \tag{4.125}$$

$$W_{TR} = \left[-\sqrt{3} \cdot \mathrm{Re}(A) - \mathrm{Im}(A) - B_e\right]/3 = -0.0173 \tag{4.126}$$

Values of compensation capacitors and inductors are calculated according Eq. (4.84)

$$\begin{aligned} C_1 &= \frac{W_{RS}}{\omega} = \frac{0.01}{314} = 3.18 \cdot 10^{-5} \\ C_2 &= \frac{W_{ST}}{\omega} = \frac{0.0173}{314} = 5.52 \cdot 10^{-5} \\ L &= -\frac{1}{\omega W_{TR}} = -\frac{1}{314 \cdot (-0.0173)} = 0.184 \end{aligned} \tag{4.127}$$

Phase currents for compensated circuit $i_R = i_S = i_T = 180.4$ A. Apparent power S and power factor PF for compensated circuit is

$$\begin{aligned} S &= \|v\| \cdot \|i\| = 10392 \cdot \sqrt{3 \cdot 180.4^2} = 3.25 \cdot 10^6 \\ PF &= \frac{P}{S} = \frac{3.24 \cdot 10^6}{3.25 \cdot 10^6} = 0.99 \end{aligned} \tag{4.128}$$

The theoretical results were confirmed by simulation. The time evolution of V_R, I_R, V_S, I_S and V_T, I_T before compensation is shown in Fig. 4.25. The same time evolution of phase's voltages and currents after compensation is shown in Fig. 4.26. The Fig. 4.27 presents time evolution of effective values of phase currents before and after connection of compensation circuit (compensation circuit was connected in time = 0.44 s)

It past hypothesis and samples was demonstrated, that direct loads with low power component, (for example, prompting engines) and unbalance can be amended with a detached system of capacitors or inductors. Nonlinear loads, for example, rectifiers, contort the current drawn from the framework. In such cases, dynamic or aloof power variable remedy might be utilized to check the twisting and raise the power element. The gadgets for redress of the power variable might be at a focal substation, spread out over a circulation framework, or incorporated with

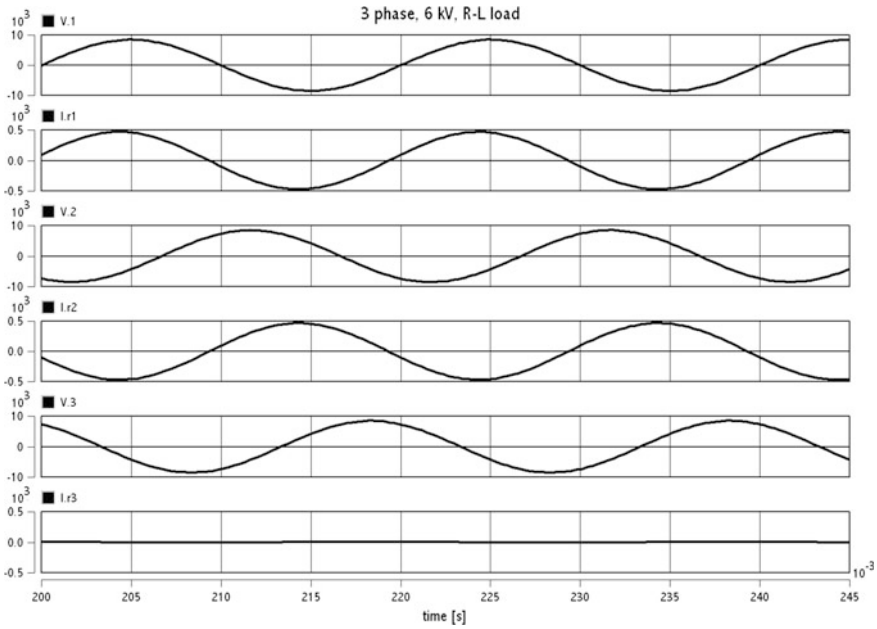

Fig. 4.25 Time evolution of voltages and currents in circuit according Example 4.5, before compensation. From *top* to *bottom*: Voltage V_R, current i_R, voltage V_S, current i_S, voltage V_T, current i_T

power devouring gear. For nonlinear load the higher harmonic are produced. These harmonics can be e.g. stifled by serial reverberation circuits.

Rather than utilizing an arrangement of exchanged capacitors for pay, an emptied synchronous engine can supply reactive power. The reactive power drawn by the synchronous engine is an element of its field excitation. This is alluded to as a synchronous condenser. It is begun and joined with the electrical system. It works at a main power variable and puts VARS (reactive energy) onto the system as required to bolster a framework's voltage or to keep up the framework power factor at a predefined level. The condenser's establishment and operation are indistinguishable to substantial electric engines. Its essential leverage is the simplicity with which the measure of remedy can be balanced; it acts like an electrically variable capacitor. Not at all like capacitors, the measure of reactive power supplied is relative to voltage (not the square of voltage), this enhances voltage security on extensive systems. Synchronous condensers are regularly utilized as a part of association with high-voltage direct-current transmission ventures or in expansive mechanical plants, for example, steel factories.

For power variable remedy of high-voltage power frameworks or huge, fluctuating modern loads, power electronic gadgets, for example, the Static VAR compensator [56, 57] or STATCOM [58, 59] are progressively utilized. These frameworks can remunerate sudden changes of power element a great deal more

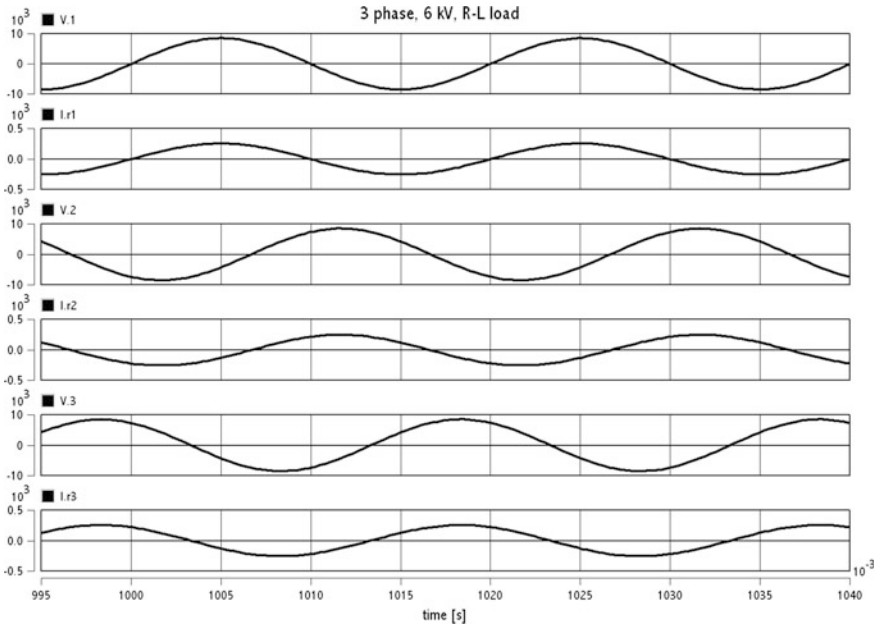

Fig. 4.26 Time evolution of voltages and currents in circuit according Example 4.5, after compensation. From *top* to *bottom*: Voltage V_R, current i_R, voltage V_S, current i_S, voltage V_T, current i_T

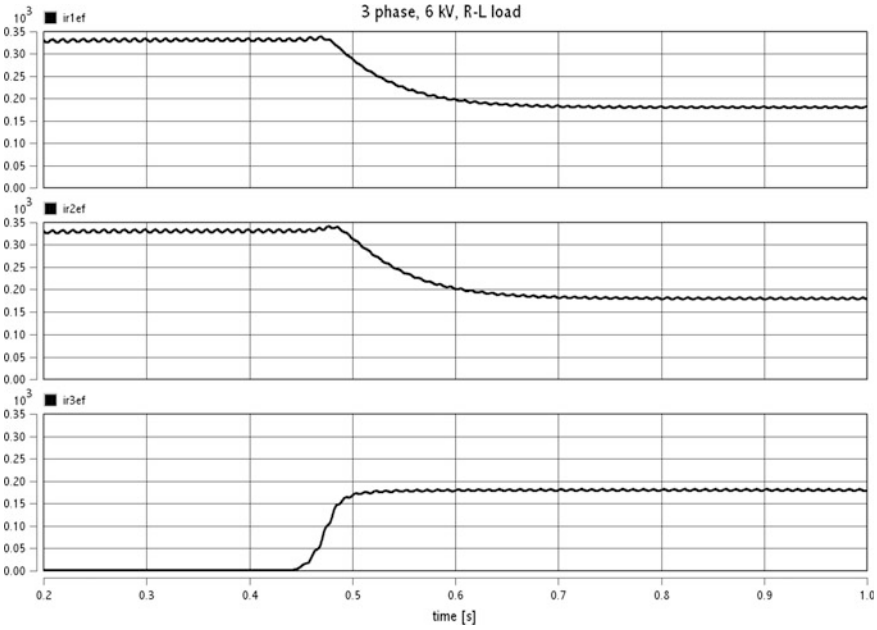

Fig. 4.27 Time evolution of RMS currents in circuit according Example 4.4, before and after compensation. Compensation parts are connected in time ≥ 0.44. From *top* to *bottom*: RMS currents i_R, i_S, i_T

quickly than contactor exchanged capacitor banks, and being strong state require less upkeep than synchronous condensers.

4.7 Quantifying of Reactive Power in Energy Meters

The sum and unpredictability of family unit electrical gear has expanded immensely in the course of the most recent couple of years. Electronic counterbalance lighting, PC screens and ventilation systems are welcome options to our homes however accompanied extra weights. One of these is on the power matrix, as these machines produce more signal harmonic.

This adjustment at last buyer profile is a hindrance for energy wholesalers which charge energy construct just with respect to dynamic power. With the use of nonlinear loads to electrical cables the dynamic energy no more speaks to the aggregate energy conveyed. As a reaction to enhance charging, the estimation of reactive energy is increasing interest.

Electromechanical meters have set a point of reference in responsive energy charging. Despite the fact that they are data transfer capacity restricted and can't consider harmonic of the line frequency, they are upheld by the worldwide standard for rotating current static VAR-hour meters for responsive energy (IEC-1268) [60]. The standard characterizes reactive energy estimations at the crucial line frequency, which suggests that it is not compulsory to incorporate harmonics. It likewise indicates extra testing conditions to check the vigor of the estimations against the third consonant, the dc counterbalance in the present data, and the line frequency variety. The different responsive power estimation routines exhibited in this chapter are assessed against these basic tests of the IEC-1268 (Table 4.1) [61].

4.7.1 Reactive Power IEEE Definition

The reactive power is well-defined in the IEEE Standard Dictionary 100-1996 under the energy "magner" as:

$$RP = \sum_{n=1}^{\infty} V_n I_n \sin(\varphi_n) \tag{4.129}$$

where V_n and I_n are respectively the voltage and current RMS values of the nth harmonics of the line frequency, and φ_n is the phase difference between the voltage and the current nth harmonics. An agreement is also adopted stating that the reactive energy should be positive for inductive load.

In an electrical framework containing absolutely sinusoidal voltage and current waveforms at a settled frequency, the estimation of reactive power is simple and can

Table 4.1 Error benchmark of different reactive energy calculation methods

Test		Power triangle	Time delay	Low pass filter
IEC 1268-reference test	Voltage and current Input *f*: $PF = 0$	Negligible	Negligible	Negligible
IEC 1268-frequency variation test	Reference test $f \pm 2\%$ and $PF = 0.87$	Negligible	5.4%	Negligible
IEC 1268-harmonic test	Reference test +10% of the third harmonics on the current signal	0.5%	Negligible	Negligible
IEC 1268-DC component test	Reference test with half way rectified sin wave on the current input	Negligible	Negligible	Negligible
Reference test +10% of the third harmonics on voltage input and 20% of the third harmonics on current input ($\varphi_1 = \varphi_2 = 30°$)		1.9%	4%	1%

be expert utilizing a few systems without blunders. In any case, in the vicinity of nonsinusoidal waveforms, the energy contained in the harmonic causes estimation blunders.

By Fourier hypothesis any occasional waveform can be composed as an aggregate of sin and cosine waves. As energy meters manage occasional signs at the line frequency both current and voltage inputs of a solitary stage meter can be portrayed by:

$$v(t) = \sum_{n=1}^{\infty} \sqrt{2} V_n \sin(n\omega_0 t) \tag{4.130}$$

$$i(t) = \sum_{n=1}^{\infty} \sqrt{2} I_n \sin(n\omega_0 t + \varphi_n) \tag{4.131}$$

where V_n, I_n are and φ_n are defined as in Eq. (4.129) and ω_0 is frequency in rad.s^{-1}.

4.7.2 Reactive Power Calculation

Method 1—Power Triangle

The Power triangle method is based on the assumption that the three energies, apparent, active and reactive, form a right-angle triangle. The reactive power can then be processed by estimating the active and apparent energies and applying:

$$RP = \sqrt{Apparent\_power^2 - Active\_power^2} \tag{4.132}$$

Despite the fact that this strategy gives amazing results with immaculate sinusoidal waveforms, perceptible mistakes show up in vicinity of harmonic (Table 4.1).

Method 2—Time Delay
A period deferral is acquainted with movement one of the waveforms by 90° at the crucial frequency and duplicate the two waveforms:

$$RP = \frac{1}{T}\int_0^T v(t) \cdot i\left(t + \frac{T}{4}\right)dt \tag{4.133}$$

where T is the period of the fundamental frequency. In an electronic DSP system, this technique can be applied by delaying the samples of one input by the quantity of samples representing a quarter-cycle of the fundamental line frequency f_{line} (Fig. 4.28).
This technique presents disadvantages if the line frequency changes and the quantity of tests no more speaks to a quarter-cycle of the crucial frequency. Huge mistakes are then acquainted with the outcomes (Table 4.1).

Method 3—Low-Pass Filter
A steady 90° phase shift over frequency with a lessening of 20 dB/decade is presented. This arrangement, which has been executed by Analog Devices, can be acknowledged with a solitary pole low-pass channel on one channel information (Fig. 4.29). On the off chance that the cut-off frequency of the low-pass channel is much lower than the central frequency, this arrangement gives a 90° phase shift at any frequency higher than the principal frequency. It likewise constricts these frequencies by 20 dB/decade. The square chart of the framework utilizing first request low-pass channel technique is appeared in Fig. 4.30.

Also to technique 2, this arrangement is defenseless to varieties of the line frequency. Be that as it may, a dynamic compensation of the addition constriction with the line frequency can be accomplished by assessing the line time of the sign (Table 4.1). As clarified above, various techniques can be utilized to figure the reactive power. The hypothetical meaning of the responsive power is hard to actualize in an electronic framework at a sensible expense. It requires a committed DSP to prepare the Hilbert change important to get a consistent stage movement of 90° at every frequency. A few arrangements have been created to beat this constraint.

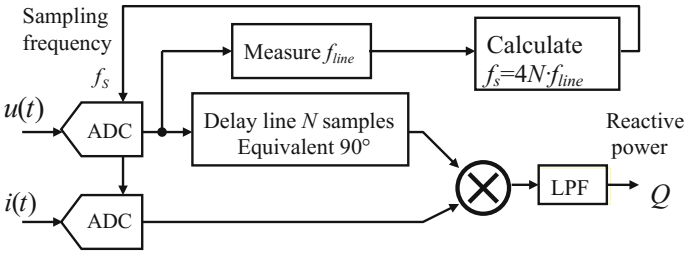

Fig. 4.28 Block diagram of the system using frequency changing compensated *T*/4 delay algorithm

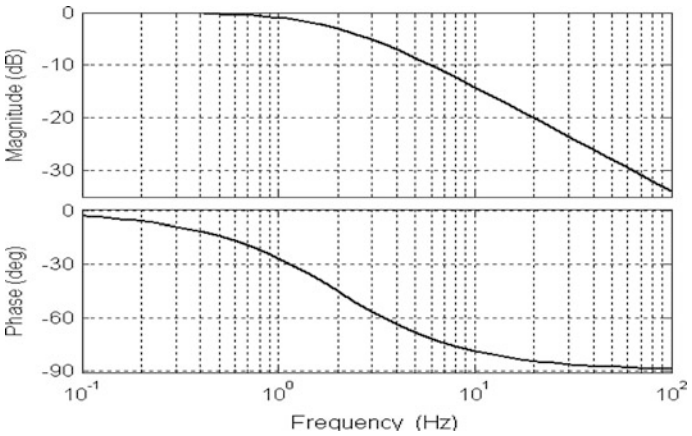

Fig. 4.29 Magnitude and phase response of low-pass filter 1st order with cutoff frequency 2 Hz

Fig. 4.30 Block diagram of the system using first order low-pass filter method

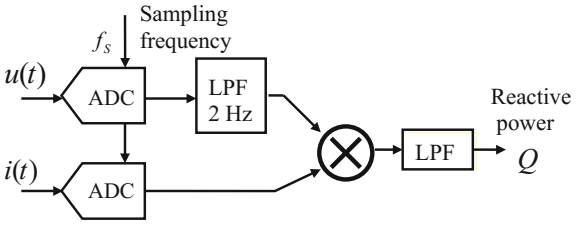

4.7.3 *Example of Integrated Circuits for Reactive Power Measuring*

The ADE7753 [62] is single-phase and ADE7854A/ADE7858A/ADE7868A/ADE7878A [63–67] are high accuracy, 3-phase electrical energy measurement ICs with serial interfaces and three flexible pulse outputs. The devices

incorporate second-order Σ–Δ analog-to-digital converters (ADCs), a digital integrator, reference circuitry, and all signal processing required to perform total (fundamental and harmonic) active, reactive (ADE7858A, ADE7868A, and ADE7878A), and apparent energy measurement and rms calculations. The ADE7878A can also perform fundamental-only active and reactive energy measurement and rms calculations.

A fixed function digital signal processor (DSP) executes the signal processing. The DSP program is stored in the internal ROM memory. The ADE7854A/ADE7858A/ADE7868A/ADE7878A can measure active, reactive, and apparent energy in various 3-phase configurations, such as wye or delta services, with both three and four wires. Aside from regular rms measurements, which are updated every 8 kHz, these devices measure low ripple rms values, which are averaged internally and updated every 1.024 s. The devices provide system calibration features for each phase, that is, rms offset correction, phase calibration, and gain calibration.

Harmonic Power Measurement with Electronic Energy Meters

Measuring Harmonic power is an important performance measure of new energy meters. Electro-mechanical meters typically measure only up to the 5th harmonic. IEC specification does not require measurement above 5th harmonic. Harmonic power has been measured in the field at up to 9.3% of the total active power up to the 50th harmonic. Accurate measurement of harmonics can be limited by the characteristics of the ADCs.

Minimum requirements for electronic meters:

Analog input bandwidth ≥ 4 kHz

ADC Sampling frequency ≥ 8ksps

With an analog input bandwidth of >4 kHz, Signals up to the 63rd harmonic will be processed correctly (in 50 and 60 Hz systems)

Tests Description and Test Results

Harmonic components in the voltage and current

Test Conditions

Channel 1 input: Sine wave at 50 Hz (140 mV) + Sine wave at 250 Hz (56 mV)

Channel 2 input: Sine wave at 50 Hz (250 mV) + Sine wave at 250 Hz (25 mV)

Reference Conditions

Channel 1 input: Sine wave at 50 Hz (140 mV)

Channel 2 input: Sine wave at 50 Hz (250 mV)

Measurement

Energy Accumulated over 4095 half line cycles (40.95 s)

Result

0.09% Error in Active Energy Measurement (IEC Limit is 0.8%)

0.46% Error in Reactive Energy Measurement

DC and even harmonics in the AC current

Half-Wave rectified waveform test (Fig. 4.31)

Test Conditions

Channel 1 input: Half wave rectified waveform at 50 Hz (300 mV)
Channel 2 input: Sine wave at 50 Hz (250 mV)

Reference Conditions

Channel 1 input: Sine wave at 50 Hz (150 mV)
Channel 2 input: Sine wave at 50 Hz (250 mV)

Measurement

Energy Accumulated over 4095 half line cycles (40.95 s)

Result

0.28% Error in Active Energy Measurement (IEC Limit is 3%)
0.27% Error in Reactive Energy Measurement (IEC Limit is 3%)

Odd harmonics in the AC current

Phase-Fired waveform test (Fig. 4.32)

Test Conditions

Channel 1 input: Phase fired rectified waveform at 50 Hz (80 mV)
Channel 2 input: Sine wave at 50 Hz (250 mV)

Reference Conditions

Channel 1 input: Sine wave at 50 Hz (40 mV)
Channel 2 input: Sine wave at 50 Hz (250 mV)

Measurement

Energy Accumulated over 4095 half line cycles (40.95 s)

Result

0.34% Error in Active Energy Measurement (IEC Limit is 3%)
0.62% Error in Reactive Energy Measurement

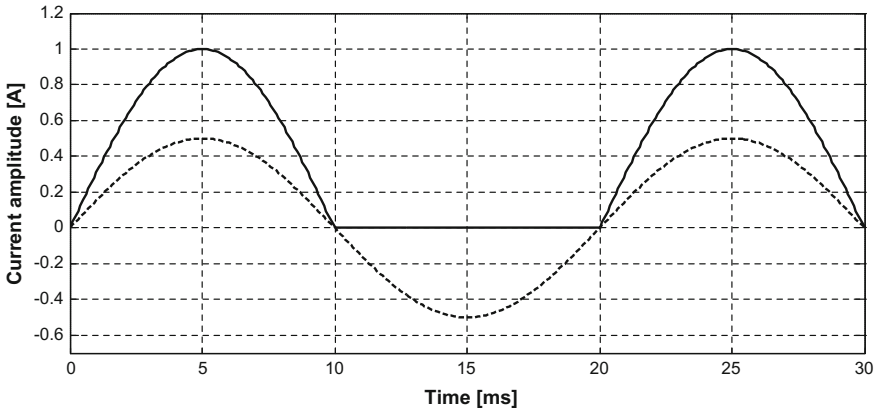

Fig. 4.31 Half-Wave rectified waveform test. *Solid line*—test waveform, *dash line*—reference waveform

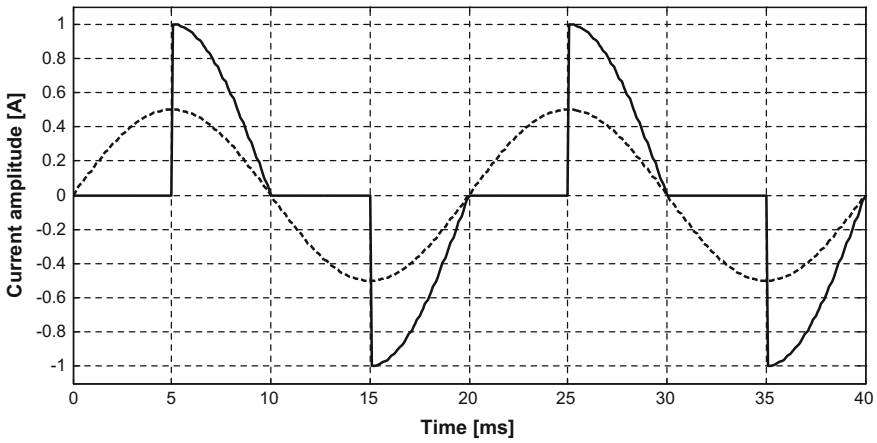

Fig. 4.32 Phase-Fired waveform test. *Solid line*—test waveform, *dash line*—reference waveform

Sub-harmonics in the AC current circuit
Burst-Fired waveform test (Fig. 4.33)
Test Conditions
Channel 1 input: Phase fired rectified waveform at 50 Hz (80 mV)
Channel 2 input: Sine wave at 50 Hz (250 mV)
Reference Conditions
Channel 1 input: Sine wave at 50 Hz (40 mV)
Channel 2 input: Sine wave at 50 Hz (250 mV)
Measurement
Energy Accumulated over 4095 half line cycles (40.95 s)
Result
0.28% Error in Active Energy Measurement (IEC Limit is 3%)
0.29% Error in Reactive Energy Measurement

4.7.4 Summary

With more nonlinear loads in family unit machines, measuring reactive energy precisely turns into a key issue for energy wholesalers. Conventional estimation techniques like the Power triangle and the Time delay com-employ with universal gauges yet indicate restrictions in the vicinity of harmonics or line frequency variety. With the most recent headways in incorporated circuit advancement, as proposed e.g. by Analog Devices, energy meter planners can now effectively actualize more exact responsive energy estimations and consequently, fulfill developing necessities from energy suppliers. The ADCs of Electronic Energy Meters should have wide enough bandwidth (>4 kHz) to measure harmonic power.

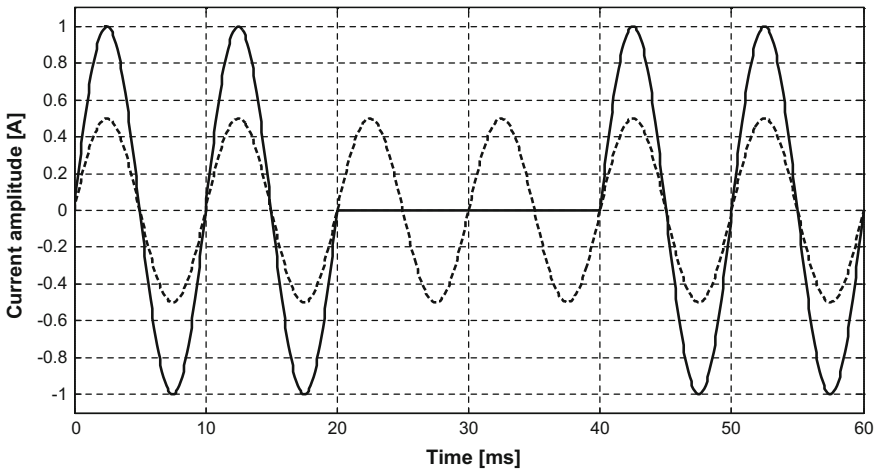

Fig. 4.33 Burst-Fired waveform test. *Solid line*—test waveform, *dash line*—reference waveform. Test waveform is on for 2 cycles and off for 2 cycles

The ADC sampling frequency should be high enough (>8 ksps) to prevent distortion of the sampled waveform. ADE products exceed the Watt-hour and VAR-hour IEC specifications for harmonic influence. The rms measurement of the ADE7753 and ADE7854A/ADE7858A/ADE7868A/ADE7878A has been proven accurate over a wide range of harmonics.

4.8 Active Power Factor Correction

An ideal Power Factor Corrector (PFC) takes from the supply V_i a current I_L which is proportional to the supply voltage as pure resistance load R_L [67–69]

$$I_L = \frac{V_i}{R_L} \tag{4.134}$$

Power factor definition—for sinusoidal input voltage

$$PF = \frac{V_1 I_1 \cos(\varphi_1)}{V_1 I_{iRMS}} = \frac{I_1}{I_{iRMS}} \cos(\varphi_1) \tag{4.135}$$

Where I_1/I_{iRMS} is distortion factor (DF) and $\cos(\varphi_1)$ is displacement factor and THD is total harmonic distortion.

$$THD = \frac{\sqrt{I_{iRMS}^2 - I_1^2}}{I_1} \tag{4.136}$$

The ideal $PF = 1$ implies:

(a) Zero phase shift between voltage and current fundamental component ($\varphi_1 = 0$)
(b) Zero current harmonic content (Fig. 4.34).

Reasons for power factor correction

(a) Increased source efficiency

- lower losses on source impedance
- lower voltage distortion (cross-coupling)
- higher power available from a given source

(b) Reduced low-frequency harmonic pollution
(c) Compliance with limiting standards (IEC 555-2, IEEE 519 etc.)

Power factor correction techniques
Passive methods: LC filters

- power factor not very high
- bulky components
- high reliability
- suitable for very small or high power levels

The easiest approach to control the harmonic current is to utilize a channel that passes current just at line frequency (50 or 60 Hz), as Fig. 4.35 [70–72]. The channel comprises of capacitors or inductors, and makes a non-direct gadget look more like a straight load. A sample of aloof PFC is a valley-fill circuit.

A detriment of latent PFC is that it requires bigger inductors or capacitors than an identical power dynamic PFC circuit [73–75]. Likewise, by and by, detached PFC is frequently less viable at enhancing the power variable [76].

Dynamic techniques: High-frequency converters

- high power factor (drawing nearer solidarity)
- probability to present a high-frequency insulating transformer
- design subordinate high-frequency harmonics era (EMI issues)
- suitable for little and medium power levels

Active PFC is the use of power electronics to adjust the waveform of current drawn by a load to progress the power factor [76]. Some kinds of the active PFC are buck, boost, buck-boost and synchronous condenser. Active power factor adjustment can be single-stage or multi-stage. In the case of a switched-mode power supply, a boost converter is placed in between the connection rectifier and the core input capacitors. The boost converter endeavors to preserve a constant DC bus voltage on its output while drawing a current that is continuously in phase with and at the same frequency as the line voltage. Another switched-mode converter inside

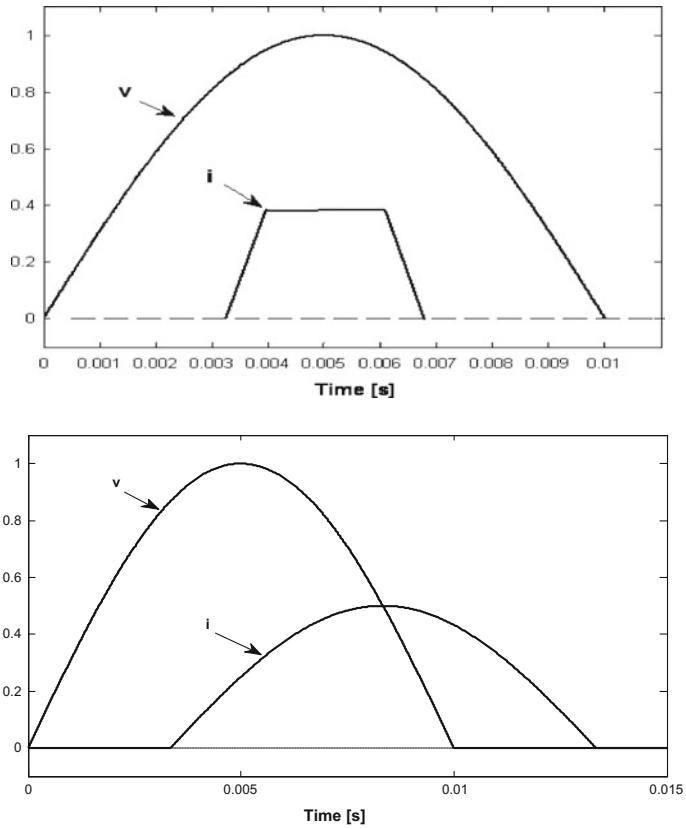

Fig. 4.34 Example of non-ideal *PF*. Zero displacement between voltage and current fundamental component (*top*), but higher harmonic in current ($\cos(\varphi_1) = 0$, $DF \neq 0$). Zero current harmonic content (*bottom*), but nonzero phase shift ($\cos(\varphi_1) \neq 0$, $DF = 0$)

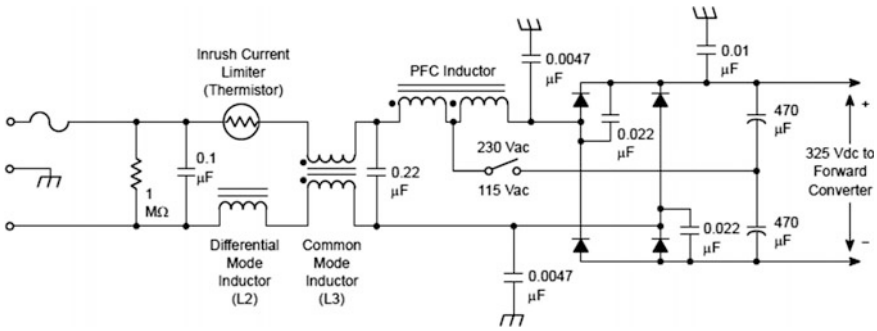

Fig. 4.35 Example of passive PFC [70, 71]

the power source produces the anticipated output voltage from the DC bus. This method necessitates extra semiconductor switches and control electronics, but permits inexpensive and minor passive components. It is regularly used in practice. Switched-mode power sources (SMPS) with passive PFC can accomplish power factor of approximately 0.7–0.75, SMPSs with active PFC, up to 0.99 power factor, while a SMPSs without any power factor rectification have a power factor of only about 0.55–0.65 [77].

Due to their very extensive input voltage range, many power supplies with active PFC can spontaneously regulate to function on AC power from about 100 V (Japan) to 230 V (Europe). That feature is principally welcome in power supplies for laptops [78–83].

Active power factor correction (DPFC), occasionally mentioned to as "real-time power factor correction," is used for electrical steadying in cases of fast load changes (e.g. at large manufacturing sites). DPFC is suitable when normal power factor correction would affect over or under correction [83] DPFC uses semiconductor switches, normally thyristors, to rapidly connect and disconnect capacitors or inductors from the grid in order to progress power factor.

Active power factor corrector

Standard conformation—Two stage PFC, Cascade connection, shown in Fig. 4.36 [68]. More detailed of block diagram of the classic PFC circuit is displayed in Fig. 4.37.

There are two ways of PFC operation; intermittent and continuous mode. Intermittent way is when the boost converter's MOSFET is turned on when the inductor current touches zero, and turned off when the inductor current encounters the anticipated input reference voltage as shown in Fig. 4.38. In this mode, the input current waveform tracks that of the input voltage, consequently reaching a power factor of near to 1 [84, 85].

Intermittent mode can be used for SMPS that have power levels of 300 W or less. Compared to continuous type equipment, discontinuous ones use greater cores and have upper RI^2 and skin effect losses due to the greater inductor current fluctuates. With the amplified swing a bigger input filter is also obligatory. On the positive cross, since discontinuous type equipment change the boost MOSFET on when the inductor current is at zero, there is no opposite retrieval current (I_{RR}) specification required on the boost diode. This means that fewer expensive diodes can be used.

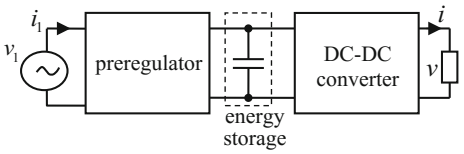

Fig. 4.36 The block diagram of two stage PFC cascade connection

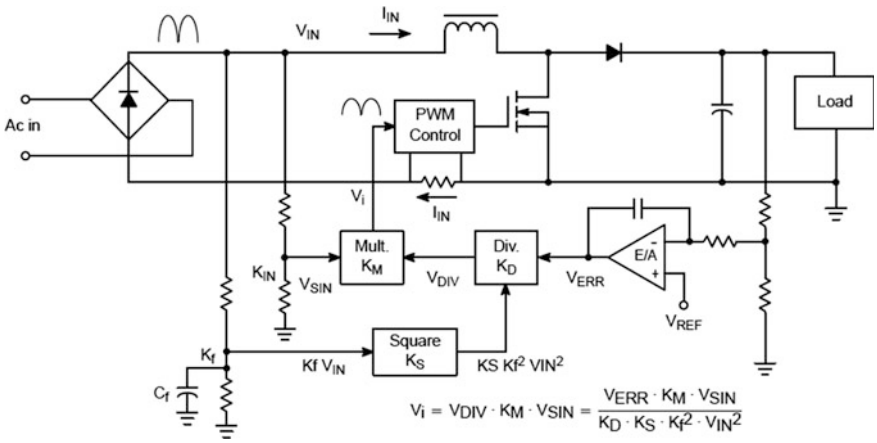

Fig. 4.37 Block diagram of the classic PFC circuit [68]

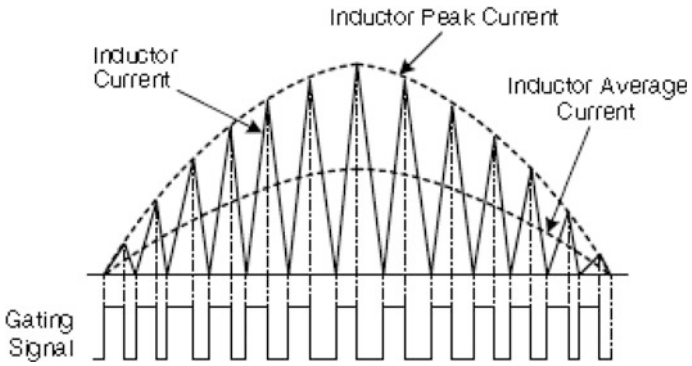

Fig. 4.38 Discontinuous mode of PFC operation

Continuous mode naturally suits SMPS power levels bigger than 300 W. This is where the boost converter's MOSFET does not switch on when the boost inductor is at zero current, in its place the current in the energy transmission inductor at no time grasps zero during the switching sequence (Fig. 4.39).

Leading Edge Modulation/Trailing Edge Modulation (LEM/TEM) versus Trailing Edge Modulation/Trailing Edge Modulation (TEM/TEM)

Leading edge/trailing edge modulation is a patented Fairchild technique to synchronize the PFC controller to the pulse-width modulation (PWM) controller [85]. Naturally TEM/TEM is used in PFC/PWM controllers which outcomes in an extra stage as well as a larger PFC bulk capacitor (as shown below).

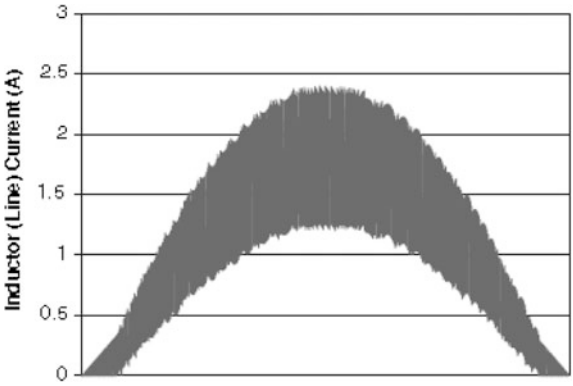

Fig. 4.39 Inductor current in continuous mode of PFC operation

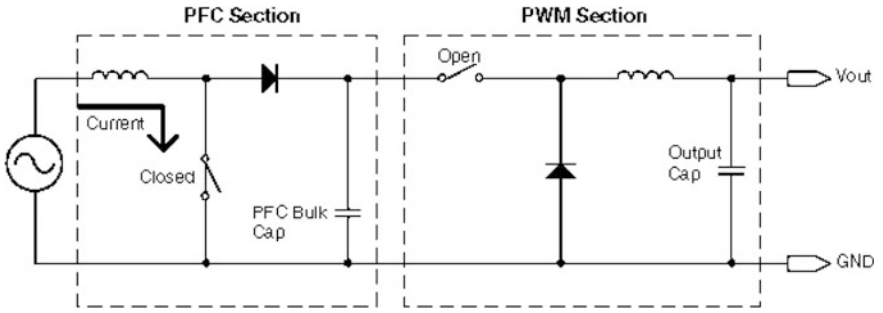

Fig. 4.40 Energizing the PFC Inductor [85]

Figure 4.40 illustrates the PFC inductor being energized. Figure 4.41 shows the energy from the inductor being transferred into the PFC bulk capacitor. When the PWM switch is shut, as shown in Fig. 4.42, the energy kept within the PFC bulk capacitor is used to drive the load. Every time this cycle is recurred, the PFC bulk capacitor has to be completely charged since it is fully discharged when the PWM switch is shut.

Fairchild Patented Leading Edge Modulation/Trailing Edge Modulation (LEM/TEM) Technique

In LET/TEM the PFC and PWM switches are tied together, but opening and closing 180° out of phase, so when the PFC switch is open the PWM switch is shut and vice versa [85]. Originally while the PFC switch is shut, the PFC inductor is energized, once the PWM switch is shut, both the output and the PFC bulk capacitor are energized. Figures 4.43 and 4.44 show that upon frequency of this

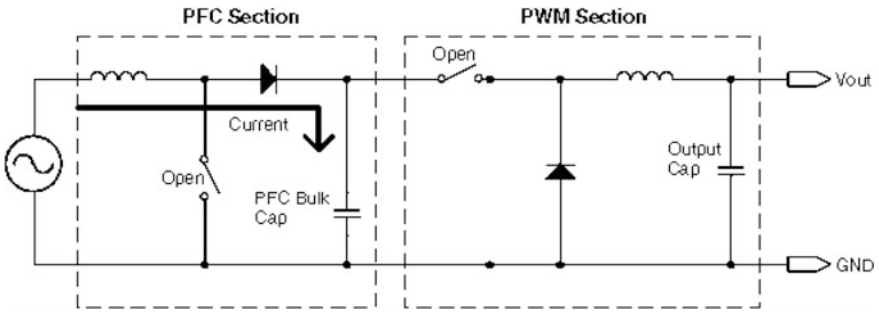

Fig. 4.41 Charging the PFC Bulk Capacitor [85]

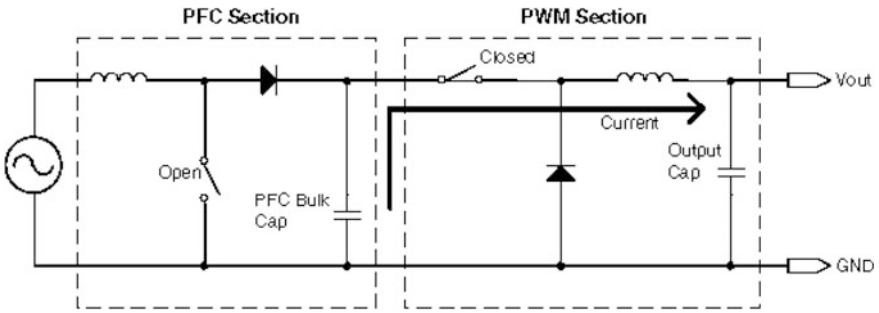

Fig. 4.42 Powering the Output [85]

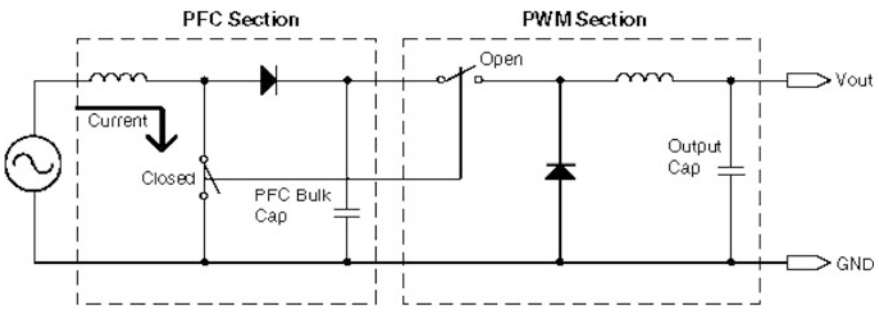

Fig. 4.43 Energizing the PFC Inductor [85]

cycle, the PFC bulk capacitor does not have to be that huge because it is not driving the output all by itself, the PFC inductor is serving out as well.

There are numerous standards in place to drive power consumption to a power factor of 1 and preserve total harmonic alteration to a minimum. Depending on the output power and the designer's requirements, a SMPS can be designed with either a discontinuous or continuous method standalone PFC controller, or a continuous

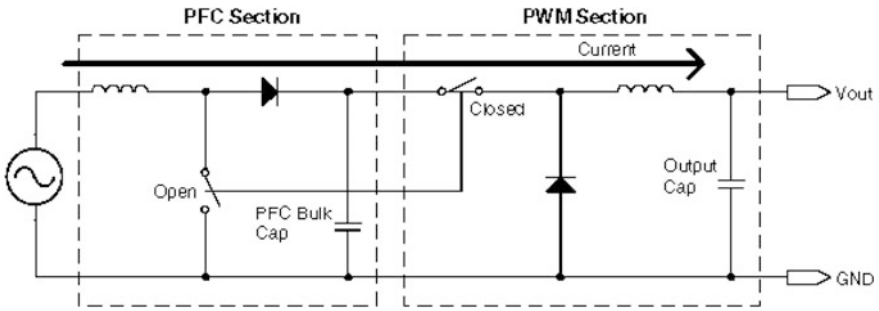

Fig. 4.44 Charging the PFC Bulk Capacitor and Powering the Output [85]

PFC/PWM mode device can be used. PFC controllers are predicted to quickly grow in near future, and standards are dropping the smallest power restrictions on systems that necessitate PFC, more and more PFC controllers will be used.

4.9 Conclusion

In this chapter the theory and principle reactive power compensation for one-phase and three-phase networks were described. On the beginning the cyclodissipativity used for reactive power compensation was presented. Results of this theory were used in several examples. It was demonstrated that the results can be used for control algorithms of automatic compensator. In the first parts of chapter the reactive power decreasing (or power factor increasing) was based on passive compensation (capacitor, inductor). The one subchapter was also devoted to digital power and energy meter description. In the last subchapter the active power filters were also described.

The main aim of this chapter was to show different principles of reactive power compensation, theory and examples which can be used for effective calculation of compensation elements.

Acknowledgements Milan Stork's participation was supported by Department of Applied Electronics and Telecommunications, University of West Bohemia, Plzen, Czech Republic and by the European Regional Development Fund and the Ministry of Education, Youth and Sports of the Czech Republic under the Regional Innovation Centre for Electrical Engineering (RICE), project No. No. LO1607, the Internal Grant Agency of University of West Bohemia in Pilsen, the project SGS-2015-002 and GA15-22712S.

References

1. V.A. Katic, Network Harmonic Pollution - A Review and Discussion of International and National Standards and Recommendations, Proc. Power Electronics Congress - CIEP, 1994, pp. 145–151.
2. T.S. Key, J.S. Lai, IEEE and International Harmonic Standard Impact on Power Electronic Equipment Design, Int. Conf. Industrial Electronics, Control and Instrumentation IECON, 1997, pp. 430–436.
3. A. Rash, Power Quality and Harmonics in the Supply Network: A Look at Common Practices and Standards, Proc. Mediterranean Electrotechnical Conf. MELECON, 1998, pp. 1219–1223.
4. IEEE PES Working Group on Nonsinusoidal Situations, A Survey of North American Electric Utility Concerns Regarding Nonsinusoidal Waveforms, IEEE Trans. Power Delivery, vol. 11, pp. 73–78, Jan. 1996.
5. A. Ferrero, Definitions of Electrical Quantities Commonly Used in Nonsinusoidal Conditions, Eur. Trans. Electric Power, vol. 8, pp. 235–240, 1998.
6. M. Depenbrock, The FBD Method, a Generally Applicable Tool for Analyzing Power Relations, IEEE Trans. Power Systems, vol. 8, pp. 381–387, May 1993.
7. M. Depenbrock, V. Staudt, The FBD Method as a Tool for Compensating Total Nonactive Currents, Proc. Int. Conf. Harmonics and Quality of Power, 1998, pp. 320–324.
8. M. Depenbrock, V. Staudt, Stability Problems if Three-Phase Systems with Bidirectional Energy Flow Are Compensated Using the FBD Method, Proc. Int. Conf. Harmonics and Quality of Power, 1998, pp. 325–330.
9. L.S. Czarnecki, Minimization of Unbalanced and Reactive Currents in Three-Phase Asymmetrical Circuits with Nonsinusoidal Voltage, Proc. Inst. Elect. Eng. B, vol. 139, pp. 347–354, 1992.
10. L.S. Czarnecki, Physical Reasons of Currents RMS Value Increase in Power Systems with Nonsinusoidal Voltage, IEEE Trans. Power Delivery, vol. 8, pp. 437–447, Jan. 1993.
11. L.S. Czarnecki, Misinterpretations of Some Power Properties of Electric Circuits, IEEE Trans. Power Delivery, vol. 9, pp. 1760–1769, Oct. 1994.
12. L.S. Czarnecki, Power related Phenomena in Three-Phase Unbalanced Systems, IEEE Trans. Power Delivery, vol. 10, pp. 1168–1176, July 1995.
13. L.S. Czarnecki, Comments on Active Power Flow and Energy Accounts in Electrical Systems with Nonsinusoidal Waveforms and Asymmetry, IEEE Trans. Power Delivery, vol. 11, pp. 1244–1250, July 1996.
14. L.S. Czarnecki, Comments, with a Reply on a New Control Philosophy for Power Electronic Converters as Fictitious Power Compensators, IEEE Trans. Power Electron., vol. 5, pp. 503–504, Oct. 1990.
15. P. Mattavelli, P. Tenti, Design Aspects of Hybrid Compensation Systems, Eur. Trans. Electric Power, vol. 8, pp. 375–382, 1998.
16. IEEE PES Working Group on Nonsinusoidal Situations, Practical Definitions for Powers in Systems with Nonsinusoidal Waveforms and Unbalanced Loads: A Discussion, IEEE Trans. Power Delivery, vol. 11, pp. 79–101, Jan. 1996.
17. E.B. Makram, S. Varadan, Definition of Power Components in the Presence of Distorted Waveforms Using Time-Domain Technique, Proc. Southeastern Symp. System Theory, 1991, pp. 536–539.
18. A. Emanuel, Apparent Power: Components and Physical Interpretation, Proc. Int. Conf. Harmonics and Quality of Power, 1998, pp. 1–13.
19. W. Shepherd, P. Zand, Energy Flow and Power Factor in Nonsinusoidal Circuits, Cambridge, U.K.: Cambridge Univ. Press, 1979.
20. N. LaWhite, M. Ilic, Vector Space Decomposition of Reactive Power for Periodic Nonsinusoidal Signals, IEEE Trans. Circuits Syst. I, vol. 44, pp. 338–346, Apr. 1997.

21. H. Akagi, Y. Kanazawa, A. Nabae, Instantaneous Reactive Power Compensators Comprising Switching Devices without Energy Storage Components, IEEE Trans. Ind. Application, vol. 20, pp. 625–630, May/June 1984.
22. F.Z. Peng, J.S. Lai, Generalized Instantaneous Reactive Power Theory for Three-Phase Power Systems, IEEE Trans. Instrum. Measur., vol. 45, pp. 293–296, Feb. 1996.
23. F.Z. Peng, G.W. Ott, D.J. Adams, Harmonic and Reactive Power Compensation Based on the Generalized Instantaneous Reactive Power Theory for Three-Phase Four-Wire Systems, IEEE Trans. Power Electron., vol. 13, pp. 1174–1181, Nov. 1998.
24. J.L. Willems, Critical Analysis of the Concepts of Instantaneous Power Current and Active Current, Eur. Trans. Electric Power, vol. 8, pp. 271–274, 1998.
25. A. Nabae, T. Tanaka, A Quasi Instantaneous Reactive Power Compensator for Unbalanced and Nonsinusoidal Three-Phase Systems, Proc. IEEE Power Electronics Specialists Conf., 1998, pp. 823–828.
26. J.H.R. Enslin, J.D. van Wyk, Measurement and Compensation of Fictitious Power under Nonsinusoidal Voltage and Current Conditions, IEEE Trans. Instrum. Measurement, vol. 37, pp. 403–408, Sept. 1988.
27. F.P. Venter, J.D. van Wyk, L. Malesani, A Comparative Evaluation of Control Strategies for Current-Fed Converters as Filters for Nonactive Power in Networks, Proc. IEEE IAS Annual Meeting, 1992, pp. 829–836.
28. P. Salmeron, J. C. Montano, Instantaneous Power Components in Polyphase Systems under Nonsinusoidal Conditions, Proc. Inst. Elect. Eng. Sci. Meas. Technol., vol. 143, pp. 151–155, 1996.
29. W. le Roux, J.D. van Wyk, Correspondence and Difference between the FBD and Czarnecki Current Decomposition Methods for Linear Loads, Eur. Trans. Electric Power, vol. 8, pp. 329–336, 1998.
30. W. le Roux, J.D. van Wyk, Evaluation of Residual Network Distortion during Compensation According to the Instantaneous Power Theory, Eur. Trans. Electric Power, vol. 8, 1998, pp. 337–344.
31. R. Gretsch, M. Neubauer, System Impedances and Background Noise in the Range 2 kHz to 9 kHz, Eur. Trans. Electric Power, vol. 8, pp. 369–374, 1998.
32. G. Blajszczak, Space Vector Control of a Unified Compensator for Nonactive Power, Proc. Inst. Elect. Eng. C, vol. 141, pp. 207–211, 1994.
33. P. Tenti, P. Mattavelli, A Time-Domain Approach to Power Term Definitions under Non-Sinusoidal Conditions, Sixth International Workshop on Power Definitions and Measurements under Non-Sinusoidal Conditions Milano, October 13–15, 2003
34. E. Tedeschi, P. Tenti, Cooperative Design and Control of Distributed Harmonic and Reactive Compensators, International School on Nonsinusoidal Currents and Compensation Lagow, Poland, 2008.
35. D. Jeltsema, E. Garcia Canseco, R. Ortega, J.M.A. Scherpen, Towards a Regulation Procedure for Instantaneous Reactive Power, 16th IFAC World Congress, Prague, Czech, July 4–8 2005.
36. E.G. Canesco, R. Grino, R. Ortega, M. Salichs, A.M. Stankovic, Power-Factor Compensation of Electrical Circuits, IEEE Control Systems Magazine, April 2007, pp. 46–59.
37. D. Luenberger, Optimization by Vector Space Methods, New York: Wiley & Sons Inc., 1969.
38. R. Ortega, E. Garcia Canseco, Inter-Connection and Damping Assignment Passivity Based Control: A Survey, European Journal of Control: Special Issue on Lagrangian and Hamiltonian Systems, vol. 10, pp. 432–450, December 2004.
39. A. Astolfi, R. Ortega, R. Sepulchre, Stabilization and Disturbance Attenuation of Nonlinear Systems Using Dissipativity Theory, European Journal of Control, vol. 8, no. 5, pp. 408–433, 2002.
40. D. Mayer, J. Hrusak, M. Stork, On State-Space Energy Based Generalization of Brayton-Moser Topological Approach to Electrical Network Decomposition, Springer, Computing, 2013.

41. D.J. Hill, P.J. Moylan, Dissipative Dynamical Systems: Basic Input-Output and State Properties, Journal of the Franklin Institute, vol. 309, no. 5, pp. 327–357, May 1980.
42. P. Penfield, R. Spence, S. Duinker, Tellegen's Theorem and Electrical Networks, MIT Press, 1970.
43. D. Jeltsema, Modeling and Control of Nonlinear Networks: A Power Based Perspective, Ph. D. dissertation, Delft University of Technology, The Netherlands, May 2005.
44. D. Jeltsema, R. Ortega, J.M.A. Scherpen, On Passivity and Power-Balance Inequalities of Nonlinear RLC Circuits, IEEE Trans. on Circuits and Systems-Fund. Theory and Appl., vol. 50, no. 9, 2003, pp. 1174–1178.
45. L.S. Czarnecki, What is Wrong with the Budeanu Concept of Reactive and Distortion Power and Why it Should Be Abandoned, IEEE Trans. on Instrumentation and Measurement, vol. IM-36, no. 3, September 1987, pp. 834–837.
46. L.S. Czarnecki, Powers in Nonsinusoidal Networks: Their Interpretation, Analysis, and Measurement, IEEE Trans. on Instrumentation and Measurement, vol. 39, no. 2, April 1990, pp. 340–345.
47. L.S. Czarnecki, Power Related Phenomena in Three-Phase Unbalanced Systems, IEEE Trans. on Power Delivery, vol. 10, no. 3, pp. 1168–1176, 1995.
48. L.S. Czarnecki, Closure on Instantaneous Reactive Power p-q Theory and Power Properties of Three-Phase Systems, IEEE Trans. on Power Delivery, vol. 23, no. 3, 2000.
49. L.S. Czarnecki, Powers and Compensation in Circuits with Periodic Voltages and Currents, Part 8: Balancing and Reactive Power Compensation of Three-Phase Linear Loads, Journal on Electrical Power Quality and Utilization, vol. 7, no. 1, 2001, pp. 9–15.
50. L.S. Czarnecki, Currents' Physical Components (CPC) in Circuits with Nonsinusoidal Voltages and Currents, Part 1: Single-Phase Linear Circuits, Electrical Power Quality and Utilization Journal, vol. XI, no. 2, 2005, pp. 27–48.
51. L.S. Czarnecki, Currents' Physical Components (CPC) in Circuits with Nonsinusoidal Voltages and Currents, Part 2: Three-Phase Three-Wire Linear Circuits, Electrical Power Quality and Utilization Journal, vol. XII, no. 1, 2006, pp. 3–13.
52. P. Tenti, J.L. Willems, P. Mattavelli, E. Tedeschi, Generalized Symmetrical Components for Periodic Non-Sinusoidal Three Phase Signals, Seventh International Workshop on Power Definition and Measurements under Nonsinusoidal Conditions, Cagliari, Italy, July 2006.
53. L.S. Czarnecki, Could Power Properties of Three-Phase Systems be Explained in Terms of the Poynting Vector?, IEEE Trans. on Power Delivery, vol. 21, no. 1, Jan. 2006, pp. 339–344.
54. E. Tedeschi, P. Tenti, P. Mattavelli, Cooperative Operation of Active Power Filters by Instantaneous Complex Power Control, Proc. of the 7th Int. Conf. on Power Electronics and Drive Systems (PEDS 07), Bangkok, Nov. 2007.
55. L.S. Czarnecki, Powers and Compensation in Circuits with Nonsinusoidal Voltages and Currents, Part 2: Current Physical Components and Compensation in LTI Circuits, On-Line Journal on Control and Electrical Engineering, vol. 1, no. 2, 2010, pp. 71–79
56. D.J. Sullivan, Improvement in Voltage and Dynamic Performance of Power Transmission System Using Static Var Compensators, BSEET, Pennsylvania State University, 1995.
57. N. Sabai, H.N. Maung, T. Win, Voltage Control and Dynamic Performance of Power Transmission System Using Static Var Compensator, World Academy of Science, Engineering and Technology, 42, 2008
58. K.K. Sen, STATCOM-Static Synchronous Compensator Theory, Modelling and Applications, IEEE PES Winter Meeting 2, 1999, pp. 1177–1183.
59. G.A. Adepoju, O.A. Komolafe, Analysis and Modelling of Static Synchronous Compensator (STATCOM): A comparison of Power Injection and Current Injection Models in Power Flow Study, International Journal of Advanced Science and Technology, vol. 36, November 2011.
60. J. Radatz, The IEEE Standard Dictionary of Electrical and Electronics Terms, Sixth Edition Standards Coordinating Committee 10, Terms and Definitions.
61. E. Moulin, Measuring Reactive Power in Energy Meters, Metering International, Issue 1, 2002, http://libvolume3.xyz/electrical/btech/semester3/electricalandelectronic-measurements/measurementofpowerandenergy/measurementofpowerandenergytutorial1.pdf

62. ADE7753 - Single-Phase Multifunction Metering IC with di/dt Sensor Interface, Analog Devices, http://www.analog.com/media/en/technical-documentation/data-sheets/ADE7753.pdf
63. ADE7854A/ADE7858A/ADE7868A/ADE7878A - Polyphase Multifunction Energy Metering IC, Analog Devices, http://www.analog.com/media/en/technicaldocumentation/data-sheets/ADE7854A_7858A_7868A_7878A.pdf
64. H. Mani, Differences Between the ADE7854A/ADE7858A/ADE7868A/ADE7878A and ADE7854/ADE7858/ADE7868/ADE7878 Products, Analog Devices, AN-1272, http://www.analog.com/media/en/technical-documentation/application-notes/AN-1272.pdf
65. Evaluating the ADE7854A/ADE7858A/ADE7868A/ADE7878A Energy Metering ICs, Analog Devices, http://www.analog.com/media/en/technical-documentation/user-guides/EVAL-ADE7878AEBZ_UG-545.pdf
66. ADE7880 - Polyphase Multifunction Energy Metering IC with Harmonic Monitoring, Analog Devices, http://www.analog.com/media/en/technical-documentation/data-sheets/ADE7880.pdf
67. ADE7816 - Six Current Channels, One Voltage Channel Energy Metering IC, Analog Devices, http://www.analog.com/media/en/technical-documentation/data-sheets/ADE7816.pdf
68. P. Tenti, G. Spiazzi, Harmonic Limiting Standards and Power Factor Correction Techniques, 6th European Conference on Power Electronics and Applications - EPE'95, 1995
69. IEEE 519 Recommended Practices and Requirements for Harmonic Control in Electrical Power Systems, IEEE Industry Applications Society/ Power Engineering Society. 1993.
70. N. Mohan, et al., Power Electronics: Converters, Applications, and Design, New York: NY, USA, John Wiley & Sons, Inc., 1995.
71. O. Garcia, J.A. Cobos, R. Prieto, P. Alou, J. Uceda, Single Phase Power Factor Correction: A Survey, IEEE Trans. Power Electron., vol. 18, no. 3, pp. 749–755, May 2003.
72. Power Factor Correction Handbook, http://www.onsemi.com/pub_link/Collateral/HBD853-D.PDF, ON Semiconductor, 2007.
73. B. Schramm, Power Supply Design Principles: Techniques and Solutions, Part 3, http://www.nuvation.com/corporate/news/newsletter/fall2006/.
74. W.H. Wolfle, W.G. Hurley, Quasi-Active Power Factor Correction with a Variable Inductive Filter: Theory, Design and Practice, IEEE Transactions on Power Electronics, vol. 18, No. 1, January 2003.
75. W.H. Wolfle, W.G. Hurley, Quasi-Active Power Factor Correction: The Role of Variable Inductance, Power Electronics, http://www.nuigalway.ie/power_electronics/projects/quasi_active.html.
76. I. Sugawara, Y. Suzuki, A. Takeuchi, T. Teshima, Experimental Studies on Active and Passive PFC Circuits, INTELEC 97, 19th International Telecommunications Energy Conference, pp. 57178, 19–23 Oct 1997, doi:10.1109/INTLEC.1997.
77. C. Chavez, J.A. Houdek, Dynamic Harmonic Mitigation and Power Factor Correction, http://dx.doi.org/10.1109/EPQU.2007.4424144, IEE Electrical Power Quality, 2007.
78. D. Adar, G. Rahav, S. Ben Yaakov, A Unified Behavioral Average Model of SEPIC Converters with Coupled Inductors, IEEE PESC'97, vol. 1, pp. 441–446, 1997.
79. V. Vorperian, Simplified Analysis of PWM Converters Using Model of PWM Switch, Parts I (CCM) and II (DCM), IEEE Trans. on Aerospace Electronic Systems, vol. 26, 1990, pp. 497–505.
80. B. Keogh, Power Factor Correction Using the Buck Topology - Efficiency Benefits and Practical Design Considerations, Texas Instruments Power Supply Design Seminar SEM1900, Topic 4 TI Literature Number: SLUP264, 2010.
81. J.P.R. Balestero, F.L. Tofoli, R.C. Fernandes, G.V. Torrico, F.J.M. de Seixas, Power Factor Correction Boost Converter Based on the Three-State Switching Cell, IEEE Trans. Ind. Electron., vol. 59, no. 3, pp. 1565–1577, Mar. 2012.
82. C. Qiao, K.M. Smedley, A Topology Survey on Single-Stage Power Factor Corrector with a Boost Type Input-Current-Shaper, IEEE Trans. Power Electron., vol. 16, no. 3, pp. 360–368, May 2011.

83. A. El Aroudi, R. Haroun, Cid-Pastor, L.M. Salamero, Suppression of Line Frequency Instabilities in PFC AC-DC Power Supplies by Feedback Notch Filtering the Pre-Regulator Output Voltage, IEEE Trans. on Circuit and Systems-I: Regular Papers, vol. 60, no. 3, March 2013.
84. Design of Power Factor Correction Using FAN7527, Application Note AN4107, Fairchild Semiconductor, http://www.fairchildsemi.com/an/AN/AN-4107.pdf, 2004.
85. Power Factor Correction (PFC) Basics, Application Note 42047, Fairchild Semiconductor, http://www.fairchildsemi.com/an/AN/AN-42047.pdf, 2004.